



HAL
open science

6-Polyamino-substituted quinolines: synthesis and multiple metal (Cu(II) , Hg(II) and Zn(II)) monitoring in aqueous media

Anton S. Abel, Alexei D. Averin, Andrey V. Cheprakov, Vitaly A. Roznyatovsky, Franck Denat, Alla Bessmertnykh-Lemeune, Irina P. Beletskaya

► To cite this version:

Anton S. Abel, Alexei D. Averin, Andrey V. Cheprakov, Vitaly A. Roznyatovsky, Franck Denat, et al.. 6-Polyamino-substituted quinolines: synthesis and multiple metal (Cu(II) , Hg(II) and Zn(II)) monitoring in aqueous media. *Organic & Biomolecular Chemistry*, 2019, 17 (17), pp.4243-4260. 10.1039/C9OB00259F . hal-02379802

HAL Id: hal-02379802

<https://hal.science/hal-02379802>

Submitted on 25 Nov 2019

HAL is a multi-disciplinary open access archive for the deposit and dissemination of scientific research documents, whether they are published or not. The documents may come from teaching and research institutions in France or abroad, or from public or private research centers.

L'archive ouverte pluridisciplinaire **HAL**, est destinée au dépôt et à la diffusion de documents scientifiques de niveau recherche, publiés ou non, émanant des établissements d'enseignement et de recherche français ou étrangers, des laboratoires publics ou privés.

6-Polyamino-Substituted Quinolines: Synthesis and Multiple Metal (Cu^{II}, Hg^{II} and Zn^{II}) Monitoring in Aqueous Media

Anton S. Abel,^{*a} Alexei D. Averin,^{a,b} Andrey V. Cheprakov,^a Vitaly A. Roznyatovsky,^a Franck Denat,^c Alla Bessmertnykh-Lemeune^{*c} and Irina P. Beletskaya^{*a,b}

Received 00th January 20xx,
Accepted 00th January 20xx

DOI: 10.1039/x0xx00000x

Chemoselective palladium-catalyzed arylation of polyamines with 6-bromoquinoline has been explored to prepare chelators for detection of metal cations in aqueous media. The introduction of a single aromatic moiety in non-protected polyamine molecules was achieved using the commercially available Pd(dba)₂/BINAP precatalyst to afford nitrogen chelators, in which aromatic signalling unit is directly attached to the polyamine residue. Water-soluble receptors were then synthesized using *N*-alkylation of these polyamines by hydrophilic coordinating residues. By combining rich photophysical properties of the 6-aminoquinoline unit with a high coordination affinity of chelating polyamines and a hydrophilic character of carboxamido-substituted phosphonic acid diesters in a single molecular device, we synthesized chemosensor **5** for selective double-channel (UV-vis and fluorescence spectroscopies) detection of Cu^{II} ions in aqueous media at physiological levels. This receptor is suitable for the analysis of drinking water and fabrication of paper test strips for the naked-eye detection of Cu^{II} ions under UV-light. By increasing the number of donor sites we also obtained chemosensor **6** which is efficient for the detection of Hg^{II} ions. Moreover, chemosensor **6** is also suitable for multiple detection of metal ions because it chelates not only Hg^{II} but also Cu^{II} and Zn^{II} ions displaying different responses of emission in the presence of these three cations.

Introduction

The development of sensitive and selective fluorescent chemosensors for application in analytic chemistry, life sciences, clinical diagnostics and environmental monitoring is an important research target of chemical analysis.¹ Besides the search for efficient molecular probes for alkali and alkali-earth metal ions, much attention has been focused on the design of small molecule indicators for d-block metal ions which should allow their efficient monitoring in industrial processes, medical analysis and toxicology, environmental and household tests.

Among the targeted hazardous metal derivatives, inorganic mercury(II) species have attracted particular attention due to their high toxicity.² Over the past hundred years, the amount of mercury in the upper 100 m layer of the world ocean has doubled. The mercury content in fish, human hair, and other biological specimens around the world is regularly reported to exceed the permitted

level. The prolonged exposure of humans to even very low concentrations of Hg^{II} can lead to neurological diseases, various cognitive and motion disorders, damage to the prenatal brain, digestive system and kidney. The maximal level established by the US Environment Protection Agency (EPA) for the content of this ion in drinking water is as low as 2 ppb (0.01 μM).³

In turn, zinc(II) and copper(II) are vital trace elements, the second and third most common in humans, respectively, and detection and imaging of these ions in biosamples are of significant interest. Zinc plays an indispensable role in various biological processes such as gene transcription, regulation of metalloenzymes, cell apoptosis, neural signal transmission, and insulin secretion, to name a few.⁴ However, the level of zinc ions in the living system should be carefully controlled because many severe neurological diseases, including cerebral ischemia, Alzheimer's disease, and epilepsy are associated with abnormal Zn^{II} levels.⁵

Copper(II) is also found in many metalloenzymes, as this metal is involved in blood formation, synthesis of hemoglobin, cytochrome, and gene expression. However, uncontrolled overloads of this element can cause serious neurodegenerative diseases.⁶ Accordingly, this metal ion is also listed by EPA among toxic substances, which should be controlled in drinking water, and its action level is fixed at 1.3 ppm (20 μM).³

When released in the environment both Zn^{II} and Cu^{II} become harmful for most living organisms.⁷ For example, excess of Zn^{II} ions may reduce the soil microbial activity and cause phytotoxic effects.⁸

Therefore, many researches were focused on the synthesis of sensors, which can detect and, in some cases, sequester these

^a Department of Chemistry, Lomonosov Moscow State University, Leninskie Gory 1-3, Moscow, 119991, Russia. E-mail: antonabel@list.ru

^b Frumkin Institute of Physical Chemistry and Electrochemistry, Russian Academy of Sciences, Leninsky Pr. 31, Moscow, 119071, Russia. E-mail: beletskaya@org.chem.msu.ru

^c Institut de Chimie Moléculaire de l'Université de Bourgogne, Université de Bourgogne Franche-Comté, UMR CRNS n° 6302, 9 Avenue Alain Savary, BP 47870, Dijon 21078 CEDEX, France. E-mail: alla.lemeune@u-bourgogne.fr

† Footnotes relating to the title and/or authors should appear here.

Electronic Supplementary Information (ESI) available: UV-vis and fluorescence spectra, NMR-spectra, DFT-calculation and structural studies details. See DOI: 10.1039/x0xx00000x

three metal ions in different environment including solutions in aqueous media under physiological conditions.⁹ Recently, the focus was moved to the development of multi-signalling (multi-channel) and/or multiple metal chemosensors which save time and effort for the synthesis of the sophisticated molecular probes.¹⁰ By using multi-modal signalling several Yes or No combinations are potentially possible leading to several signalling patterns. Different analytes can switch on different signalling channel, giving a possibility to multiple accumulation of information. Therefore, multi-modal receptors are expected to show an enhanced selectivity and anti-interference ability, to increase the detection reliability and simplify quantitative measurements. Using these detectors should also provide an increase in a working range of metal ion concentrations as chromogenic, luminescent and electrochemical signalling events are observed at different concentration levels of the analyte. However, the reported molecular probes suffer from serious limitations, such as laborious synthesis, low sensitivity, lack of selectivity, low water solubility, operational complexity and difficulties in real-time monitoring. Therefore, the development of optical detection methods, ranging from simple semi-quantitative to highly precise and sensitive ones is required for the efficient analysis of different metal cations under real-life conditions.

The development of chemosensors is laborious and time-consuming. Once the fluorophore unit has been chosen, a series of molecular probes with different ionophores need be prepared because solubility and coordination properties of the ligands are difficult to predict. In such a case, synthetic methods allowing to synthesize small libraries of molecular probes are useful. For example, conventional click chemistry reactions were reported as a rational synthetic approach to explore polymeric sensors.¹¹ We have recently proposed an efficient synthetic strategy to obtain water-soluble optical chemosensors (Scheme 1).¹²

According to this approach, the libraries of chromogenic polyamines can be synthesized from polyamines and aromatic halides *via* the chemoselective palladium-catalyzed amination reaction (Step 1) followed by the *N*-alkylation of the obtained products with different alkyl halides bearing additional coordination sites such as hydrophilic [(2-bromoacetyl)amino]methyl]phosphonic acid diethyl ester (**1**) (Step 2). Taking into account a large substrate scope of the catalytic and *N*-alkylation reactions, this strategy is expected to be efficient for search of novel chemosensors involving unusual fluoro- and ionophore units. In this work, we address the

synthesis and application of 6-aminoquinolines for double-channel detection or signalling multiple metal ions.

Aminoquinolines have attracted considerable attention in fluorescent sensing due to their rich photophysical properties, photostability, non-toxicity for non-cancer cells and high membrane permeability.^{9a,13} Depending on the position of amino group in quinoline rings, and structural parameters of the receptor unit, these compounds can afford photochemical molecular devices, which detect the presence of metal ions according to different mechanisms such as photon-induced electron transfer (PET),¹⁴ internal charge transfer (ICT),¹⁵ fluorescence resonance energy transfer (FRET),¹⁶ excited-state intramolecular proton transfer (ESIPT)¹⁷ and excimer formation.^{16,18} Thus, these compounds seem to be well suited to develop multiple-metal and multi-modal chemosensors. Surprisingly, only 8-aminoquinolines¹⁹ have been so far widely investigated in this area, with most of the reported studies being devoted to Zn^{II} ions sensing.²⁰ The potential of other positional isomers of the aminoquinolines for sensing various analytes scarcely explored and understood.^{15a,18,21}

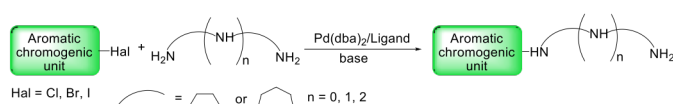
In this work we chose to explore polar 6-aminoquinolines which are interesting due to their ICT character (heterocyclic nitrogen atom serves as an electron acceptor while the amino group is an electron donor), the emission in visible region, low toxicity and good photostability.²² Despite the long-lasting interest to 6-aminoquinolines as fluorescent derivatization agents for the analysis of mono- and oligosaccharides²³ and fatty acids,²⁴ signalling reagents for C–C bond formation²⁵ or enzyme activity,²⁶ the sensory properties of these compounds are less investigated.

Shiff-base derivatives of 6-aminoquinoline have been found to be ratiometric fluorescent pH-sensitive probes.²⁷ 6-Aminoquinolines bearing carboxamide, urea or thiourea groups were found to be efficient for monitoring inorganic anions and nucleoside triphosphates.²⁸ In turn, 2-methyl-6-aminoquinolines with various *N*-substituents were proposed as chemosensors for diethylchlorophosphate, a nerve agent mimic.^{22c}

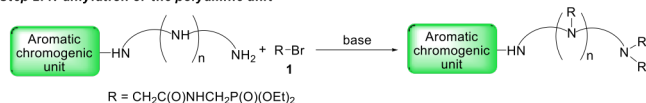
Two recent examples of the detection of metal ions by 6-aminoquinoline derivatives are of particular interest. Chemosensor **2** (Fig. 1) was proposed for highly sensitive detection of Al^{III} and Zn^{II} ions in aqueous media by UV–vis and fluorescence spectroscopies. However, these ions can be distinguished only by absorption, because the enhancement of the emission was rather similar for both of them.¹⁰ⁱ A simple colorimetric receptor **3** in acetonitrile solutions exhibited different colour changes in the presence of Hg^{II} or Cu^{II} ions.²⁹ Nevertheless, these ions also cannot be identified by fluorescence spectroscopy because each of them lead to similar emission quenching. The selectivity of the chemosensor **2** and **3** seems to be rather poor when both studied ions are present in the same solution.

It is to be noted that 6-amino group was also introduced to improve the optical response of 4-alkoxy and 4-aminoquinoline derivatives.³⁰ Moreover, oxazamacrocycles containing 4,6-diaminoquinoline fragment demonstrated interesting changes of selectivity when the structure of macrocycle was varied.³¹ The compound **4** was identified as a selective chemosensor for Cu^{II} ions in acetonitrile.

Step 1: Selective arylation of polyamines



Step 2: N-alkylation of the polyamine unit



Scheme 1. Synthetic approach to polyamine chemosensors.

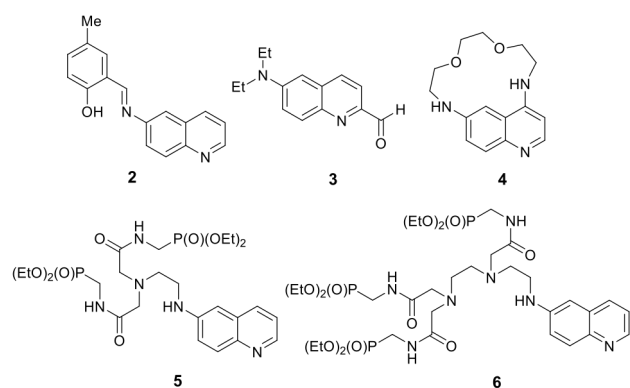


Figure 1. Chemosensors based on 6-aminoquinoline signalling units: previously reported compounds **2–4** and receptors **5** and **6** investigated in this work.

In this work, we synthesized a novel type of 6-quinolyl chemosensors with the electron-donor amino group directly attached to the heterocycle and the second one separated from the chromophore by the ethylene spacer (compounds **5** and **6**, Fig. 1). This structural organization of the receptor unit could be profitable to combine PET and ICT processes within a single sensor system as it was previously demonstrated for pH,³² anions³³ and metal ion³⁴ sensors bearing various fluorophores. Exploring sensory properties of these compounds, we revealed that chemosensor **5** was suitable for selective detection of cupric cations in aqueous medium under physiological conditions by using both UV–vis and fluorescence spectroscopies (a double-channel chemosensor). In contrast, chemosensor **6** is useful for the fluorescent detection of Hg^{II} ions. Moreover, this compound can fluorimetrically distinguish three metal ions (Cu^{II}, Zn^{II} and Hg^{II}) in aqueous media (a three-metal chemosensor). These are the first examples of 6-aminoquinolines suitable for selective and sensitive detection of toxic metal ions in physiological conditions.

Results and discussion

Ligand synthesis

The chemoselective palladium-catalyzed heterocoupling of aromatic halides with non-protected linear polyamines, in which only the primary amino groups are reactive, is a known methodology (Scheme 1).³⁵ When the reaction is carried out in the presence of excess of polyamine, selective monoarylation of the latter is observed. This reaction is useful for the synthesis of optical chemosensors, because polyamines are excellent ionophores and most of the known signalling units are derived from aromatic compounds. However, recent studies have shown that the Pd-catalyzed amination of azaheterocyclic halides is much more complicated compared to the reaction of aryl halides due to unfavorable coordination of the heterocyclic nitrogen atom to the palladium centre which can result in catalyst inactivation.^{12b,31,36}

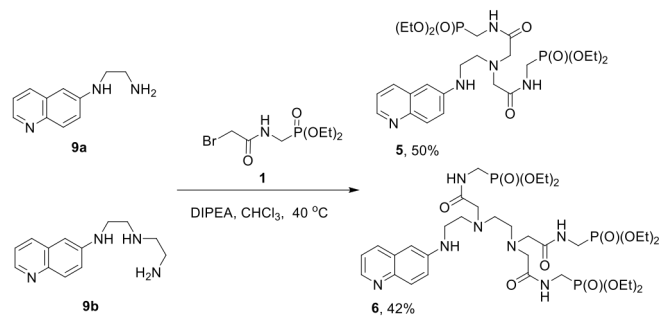
Fortunately, the reaction of 6-bromoquinoline (**7**) with polyamines **8a–f** takes place smoothly under the standard conditions, in the presence of commercially available precatalyst Pd(dba)₂/BINAP (4/4.5 mol %) and sodium *tert*-butoxide in 1,4-

Table 1. Synthesis of 6-quinolyl-substituted polyamines **9a–f**.^a

Entry	Polyamine (equiv)	Product	Yield, ^b (%)
1 ^c	(10)		75
2	(3)		62
3	(3)		40
4	(3)		45
5	(3)		57
6 ^d	(1)		37

^a Reaction conditions: 0.5 mmol of bromide **7**, polyamine, Pd(dba)₂/BINAP (4/4.5 mol%), sodium *tert*-butoxide (0.75 mmol) were refluxed in dioxane (C(**7**) = 0.1 M) under argon. ^b Isolated yield. ^c The yield of the product was 28% when 6-bromoquinoline was replaced by 6-chloroquinoline. ^d 8/9 mol% of Pd(dba)₂/BINAP were used.

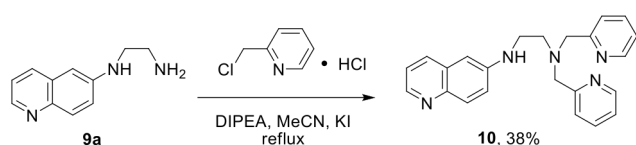
dioxane on reflux (Table 1). To obtain *N*-(6-quinolyl)-1,2-diaminoethane (**9a**) in 75% yield, the reaction of bromide **7** and 1,2-diaminoethane (**8a**) was carried out using 10 equiv of the amine (entry 1). 6-Chloroquinoline was less reactive compared to bromo derivative and the product was isolated in only 28%. Linear polyamines **8b** and **8c** bearing two or three diaminoethane moieties afforded the monoarylated products **9b** and **9c** in lower yields, 62% and 40%, respectively, with 3 equiv of polyamines employed (entries 2 and 3). The increase of loading of compounds **8b** and **8c** up to 10 equiv did not have any beneficial effect on the product yield. When triamine **8d** with longer alkyl chains was reacted with bromide **7**, the product was formed in 45% yield (entry 4). Interestingly, tris(2-aminoethyl)amine (**8e**), known as an excellent tetradentate chelator of transition-metal ions, afforded 6-quinolyl-substituted amine **9e** in 57% yield (entry 5), comparable to that observed in the reaction of bis(2-aminoethyl)amine **8b**

Scheme 2. Synthesis of chelators **5** and **6**.

(entry 2). The arylation of azamacrocycle **8f** bearing an external primary amino group gave the product only in 37% yield even when the Pd(dba)₂/BINAP catalyst loading was increased up to 8/9 mol% presumably due to high metal-chelating affinity of the tetraazamacrocycle (entry 6). To note, this reaction can be conducted using a stoichiometric amount of the expensive amine **8f** because this polyamine molecule contains a single primary amino group.

Accordingly, the scope of the reaction is quite broad and the monoarylated products can be obtained in good yields which sometimes exceeded 50%. Cu-catalyzed reaction of non-protecting polyamines with 6-bromoquinoline was reported previously,³⁷ but the selectivity of this coupling was found to be low and depend on the structure of the amines presumably due to the complexation of copper ions with polyamine chelators. In contrast, the Pd-catalyzed approach is useful for the synthesis of novel molecular probes. For example, compounds **9a–f** are of particular interest for assaying metal ions in aqueous solutions as nitrogen atoms of the polyamine chain can be further modified in view of adjusting coordination properties and enhancing sensors solubility in aqueous media. Moreover, the high reactivity of primary and secondary amino groups should provide a selective functionalization of these sites in the presence of the less reactive bulky aromatic amino group and the nitrogen atom of quinoline residue. In this work, the *N*-alkylation reaction was investigated to prepare novel hydrophilic multidentate chelators.

The parent polyamines **9a**, **9b** and **9e** were first reacted with diethyl ((bromoacetyl)amino)methyl)phosphonate (**1**) (Scheme 2). In each reaction, we used as many equivalents of bromide **1** as required for the transformation of all aliphatic amino groups into tertiary amine sites. However, classical *N*-alkylation reaction is well known for low selectivity due to competing overalkylation affording quarternary ammonium salts, which obviously lowered the yields of the target derivatives. The simplicity of procedure and ease of separation of side quarternary salts could outweigh this drawback. When triamine **9b** was reacted with bromide **1** (3.3

Scheme 3. Synthesis of compound **10**.Table 2. Photophysical data for compounds **5**, **6** and **10**.

Ligand	λ_{abs} , nm (ϵ , cm ⁻¹ M ⁻¹)	λ_{exc} , nm	H ₂ O (pH = 7.4)		CH ₃ CN	
			λ_{em} , nm	Φ^a	λ_{em} , nm	Φ^a
5	285 (4900), 356 (3200)	356	467, 554	0.012	430	0.30
6	289 (5000), 356 (3200)	356	467, 554	0.017	430	0.36
10	288 (5600), 350 (3000)	350	516	0.013	434	0.27

^a Quantum yields were measured using quinine sulfate as a standard.

^b 0.03 M HEPES solution at pH = 7.4

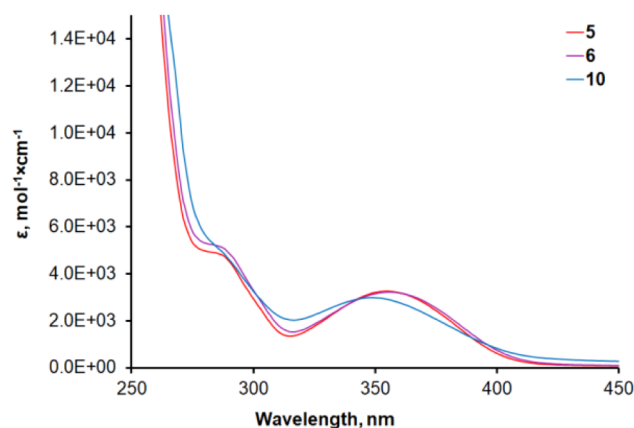
equiv) in boiling acetonitrile using K₂CO₃ as base, the target product **6** was isolated in only 26% yield. After optimizing the reaction conditions (use of DIPEA instead of potassium carbonate and running the reaction in chloroform at 40 °C), the product yield increased in this case to 42%. Under the similar conditions, the *N*-alkylation of diamine **9a** with bromide **1** (2.2 equiv) afforded compound **5** in 50% yield. However, the reaction of **1** (4.4 equiv) with polyamine **9e** bearing a tertiary amino group was too complicated and led to an inseparable mixture of tri-, tetra- and penta-functionalized derivatives.

Next, we obtained compound **10** containing two 2-picolyl fragments. This reaction also suffered from side-reactions and overalkylation. After optimization of the reaction conditions, the best yield (38%) was obtained when the reaction was performed in boiling acetonitrile in the presence of DIPEA and potassium iodide as shown in Scheme 3.

All the new compounds were unambiguously characterized by NMR, ESI-MS, IR spectra and obtained spectral data were in good agreement with the assigned structures (see ESI).

Spectroscopic studies of ligands

Phosphonate-substituted derivatives **5** and **6** were soluble in water at pH 1–12 and in 0.03 M HEPES solution under physiological conditions (pH = 7.4). In contrast, quinoline **10** was insoluble in neat

Figure 2. Electronic absorption spectrum of ligands **5**, **6** and **10** in 0.03 M HEPES solution at pH = 7.4.

water. To obtain its aqueous solutions for spectroscopic investigations, a stock solution of the ligand in methanol was prepared and diluted by water or the HEPES buffer by up to 50 times (2 vol% of methanol remained in the final solutions).

The spectroscopic data of polyamines **5**, **6** and **10** in 0.03 M HEPES solution are summarized in Table 2.

The absorption spectra of compounds **5** and **6** were almost identical and show bands characteristic of 6-aminoquinoline chromophore with absorbance maxima at 288 and 350 nm (Fig. 2).^{22a} The maximum of the low-energy band was blue-shifted in the spectrum of compound **10** by 6 nm. We assumed that it is caused by partial protonation of compound **10** in the studied solution that was further proven by detailed studies of the ligand protonation (see below).

The emission of 10^{-5} M aqueous solution of these compounds was quite low and covered a wide spectral region from 400 to 600 nm. Two bands were observed in each spectrum being better resolved in the spectrum of compound **5** (Fig. S1). The shape of bands and quantum yields were not dependent on concentration within the limits of experiment that is indicative of the absence of aggregation phenomena and excimer formation.

Protonation of ligands

Polyamines are known as excellent chelators for metal ions, and they are widely explored as ionophores in optical chemosensors.¹ However, due to rather high basicity polyamines undergo partial protonation when used in aqueous media. This process sophisticates the interpretation of data on complexation of metal ions, and should be explicitly taken into consideration.³² Thus, providing of the balance between basicity and complexing ability of

the chelator by “tuning” of the structure is quite important for chemosensor development.

The protonation of ligands **5**, **6** and **10** in aqueous solutions in a range of pH values was investigated by UV-vis and fluorescence spectroscopies. Titrations of compounds **5** and **6** were conducted in water, while the addition of a small amount of methanol (up to 6 vol% of MeOH) was necessary in the measurements of compound **10** because of its limited solubility in neat water.

Both absorption and emission of studied compounds progressively changed on gradual addition of hydrochloric acid. The spectral changes were rather similar for all compounds and representative UV-vis and fluorescence-based titrations of compound **5** are depicted in Fig. 3A and 3B, respectively. As shown in Fig. 3A, a broad absorption band was observed in basic media ($\lambda_{\text{max}} = 355$ nm). The addition of hydrochloric acid results first in the red shift of maximum to 411 nm until pH = 3.5, and then to smaller blue shift to 395 nm at higher acidities, pH lower than 2.

To determine apparent protonation constants, numerical data fitting was performed using the Specfit program.³⁸ The obtained values are compiled in Table 3 together with the literature data for the earlier reported chemosensors **11–13** involving similar ionophore units (Fig. 4).

The best fits were obtained when the UV-vis titration curves were processed with a 3-species model ($L-LH^+-LH_2^{2+}$) for polyamines **5** and **6**, and a 4-species model ($L-LH^+-LH_2^{2+}-LH_3^{3+}$) for picolyl-substituted compound **10**. Titration curves and distribution diagrams, simulated electronic absorption spectra of all studied compounds and their protonated forms calculated using the Specfit program are shown in Fig. S2–S13 (ESI[†]).

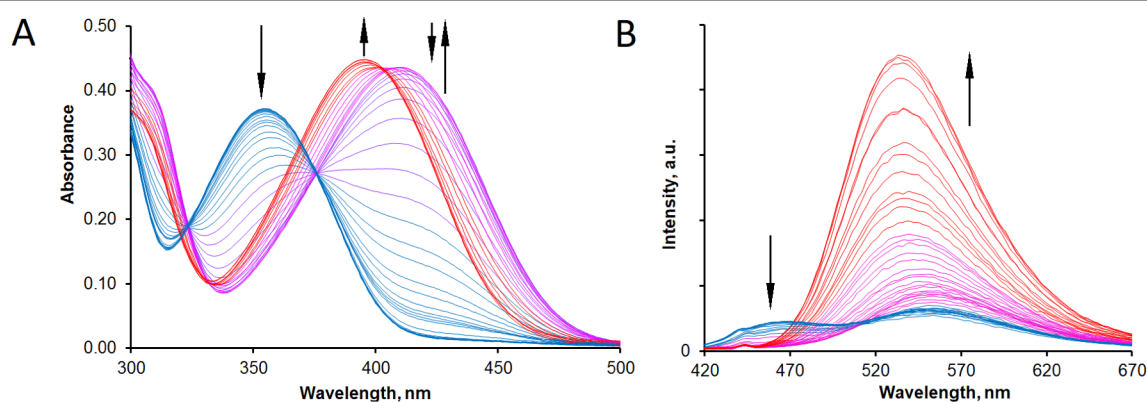


Figure 3. A) pH dependence of electronic absorption spectrum of polyamine **5**; H₂O, [5] = 133 μ M, I = 0.1 M KCl, pH = 0.7–10.2; B) pH dependence of fluorescence emission spectrum of polyamine **5**; H₂O [5] = 27 μ M, I = 0.1 M KCl, $\lambda_{\text{ex}} = 375$ nm, pH = 0.5–11.8.

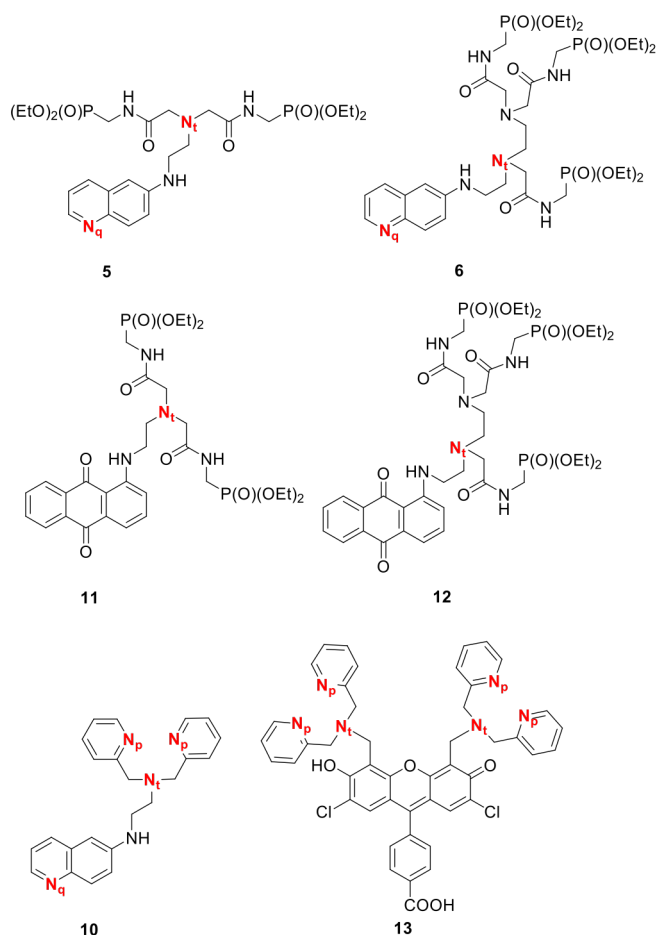


Figure 4. Labelling scheme for nitrogen atoms in chemosensors **5**, **6** and **10–13**.

The protonation sequence can be unambiguously established based on electronic absorption data (Schemes S1 and S2, Figs. S4 and S8). Moreover, the lower basicity of tertiary nitrogen atoms in carboxamide-substituted polyamines **11** and **12** was previously reported.³⁹ In agreement with these data, the protonation sequence of compounds **5** and **6** starts from the quinoline nitrogen atom (N_q) that induces a large bathochromic shift of the absorption maximum of compounds **5** and **6**. The next proton is likely to go to the tertiary nitrogen atom (N_t) bearing lesser number of electron-withdrawing carbamoylmethyl substituents. This protonation step is observed at significantly different pH for compounds **5** and **6**, in full agreement with higher basicity of nitrogen with a single electron-withdrawing substituent, as compared to the atom bearing two of such. However, spectral changes corresponding to this step are small and similar for both compounds because the protonation of nitrogen atoms remote from the chromophore very slightly affects the absorption properties of the compounds.

The assignment of the protonation sites of ligand **6** was also confirmed by ^1H and $^{31}\text{P}\{^1\text{H}\}$ NMR experiments (Fig. S26 and S27). First, the ^1H and $^{31}\text{P}\{^1\text{H}\}$ NMR spectra of 0.04 M solution of polyamine **6** in a $\text{D}_2\text{O}/\text{MeOH}-d_4$ mixture (5:1) were recorded, and all proton signals were assigned. Then, this solution was acidified to pH = 2 and ^1H and $^{31}\text{P}\{^1\text{H}\}$ NMR spectra were recorded again. Spectral changes in proton and phosphorous chemical shifts were in a good

Table 3. Apparent stepwise protonation of polyamines **5**, **6** and **10** and relevant compounds **11–13**^a reported in the literature.

Ligand	Method	pKa(N_q)	pKa(N_t)	pKa(N_p)
5 ^b	(FL) ^e	5.60(5)	2.23(1)	–
	(UV-vis) ^f	5.64(1)	2.26(4)	–
6 ^b	(FL) ^e	6.2(1)	4.38(2)	–
	(UV-vis) ^f	5.51(4)	4.4(1)	–
10 ^b	(FL) ^e	5.18(6)	6.82(7)	3.91(3)
	(UV-vis) ^f	5.25(9)	6.8(2)	3.2(3)
11 ^c	(UV-vis) ^f	–	2.11(1)	–
12 ^c	(UV-vis) ^f	–	4.39(3)	–
13 ^d	(PT) ^h	–	6.96(1)	3.81(3)

^a Structures of the ligands and the labeling scheme of nitrogen atoms are depicted in Fig. 4. ^b I = 0.1 M KCl, T = 298(2) °C

^c Ref. ³⁹. ^d Ref. ⁴⁰. ^e Fluorescence measurements. ^f UV-vis spectrophotometric measurements. ^h Potentiometric measurements.

agreement with the structure of diprotonated species proposed during the interpretation of UV-vis data (Scheme S2).

The calculated absorption spectra of polyamine **10** and its monoprotinated form $[\mathbf{10H}]^+$ are similar (Fig. S12). Thus, the first proton should mainly reside on the tertiary nitrogen atom (N_t) which is the most basic, being the most distant from 6-aminoquinoline chromophore (Scheme S3). The second protonation resulted in bathochromic shifts and hyperchromic change of the absorption band, suggesting protonation affecting the quinoline nitrogen atom (N_q). In the third step, the pyridine nitrogen atoms (N_p) are protonated, leaving the chromophore almost unaffected as evidenced by close resemblance of the absorption spectra of $[\mathbf{10H}_2]^{2+}$ and $[\mathbf{10H}_3]^{3+}$.

In the visible region of fluorescence spectra of ligands **5**, **6** and **10**, two very broad emission bands were observed under basic conditions (Figs. 3B, S18 and S22). When pH was decreased from 11 to 7 by adding hydrochloric acid, the spectral changes were small. However, acidification of the solution towards pH = 3–4 leads to a disappearance of the higher-energy band (467 nm for **5**) with simultaneous increase of the intensity of the second band (554 nm for **5**). Then a blue shift of the emission band maxima (536 nm for **5**) was observed and the maximal degree of "turn-on" observed on further acidification of the solution. Thus, the examination of pH dependence of fluorescence spectra of these compounds showed switching on of emission upon protonation of the side-chain amine presumably as a result of thermodynamically less favorable PET process involving the side nitrogen atom (N_t) separated from aminoquinoline fragment by two methylene units.³² Moreover, the shape of the emission spectrum and the positions of the maxima

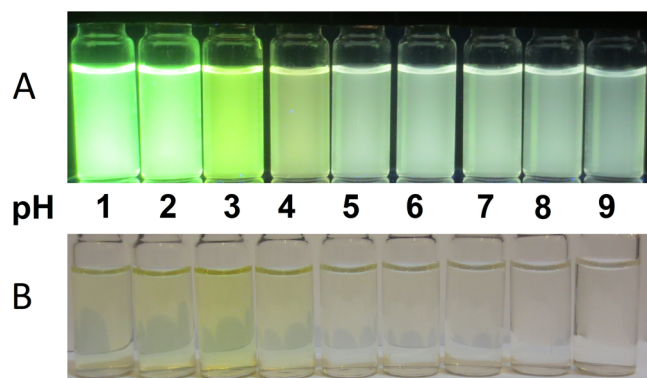


Figure 5. Color evolution of aqueous solution of ligand **5** with pH increase observed under UV ($\lambda = 356$ nm) (A) and visible (B) light.

change during the titration that presumably indicates a significant contribution of the emission according to internal charge transfer (ICT) mechanism. Excited species in this case are highly responsive to protonation of the quinoline nitrogen atom and intramolecular hydrogen bonding of the aromatic 6-amino group.

The respective apparent protonation constants were estimated using the Specfit program (Figs. S18–S25). As in the UV–vis titrations, the 3-species model ($L-LH^+-LH_2^{2+}$) was used for polyamines **5** and **6** and a 4-species model ($L-LH^+-LH_2^{2+}-LH_3^{3+}$) for picolyl-substituted derivative **10**. The obtained values of the constants are reported in Table 3. These values are in a good agreement with those derived from spectrophotometric titrations.

As shown in Fig. 5 for compound **5**, the colour of the ligand solution changes at pH = 3–4 after the protonation of quinoline nitrogen. This change can be observed by naked eye and is particularly well visible under UV-light, when the colour of emission serves as a backlit background for the observation of yellow tint of solution.

Thus, compounds **5**, **6** and **10** can be regarded as suitable dyes for spectroscopic monitoring of pH. Moreover, the protonation of all studied chelators is observed only at pH < 8 due to electron-withdrawing character of substituents attached to the aliphatic amino groups. The lower basicity of these compounds is favourable for the study of binding metal cations in aqueous media, in which the competitive protonation of the ligand is an unfavourable sophistication. From this point of view, the valuable property of the carboxamide substituent compared to the 2-picolyl fragment is its ability to decrease the pK_a values of the binding pockets thereby extending the pH interval favourable for binding metal ions up to physiological conditions.

Detection of metal cations

The sensing properties of receptors **5**, **6** and **10** were evaluated by UV–vis and fluorescence spectroscopy. The spectra were recorded before and after addition of excess (5 equiv) of 15 metal perchlorates to aqueous solutions of the ligands at pH = 7.4 maintained with HEPES buffer.

Ligand **10** in which the diamine chain is functionalized by two 2-picolyl residues exhibits low selectivity with respect to environmentally-relevant metal ions. Remarkable absorbance changes were observed after addition of Zn^{II} , Cd^{II} , Cu^{II} , Co^{II} and Ni^{II} ions to the ligand solution (Fig. S28). Emission of the ligand also changed in the presence of these cations (Fig S29). Our attempts to increase the chelator selectivity by switching from HEPES to acetate buffer (pH = 5.0) where **10** exists in protonated forms (Fig S13) failed. In acetate buffer, the spectral response was observed for nine different cations as shown in Fig. S30 and S31.

Sensing properties of diamine **5** differ from those of chelator **10**. Spectral investigations of the solutions before and after addition of 15 different metal perchlorates showed remarkable hypsochromic shifts of absorption bands of chemosensor **5** only after addition of Cu^{II} ions (Fig. 6 and S32).

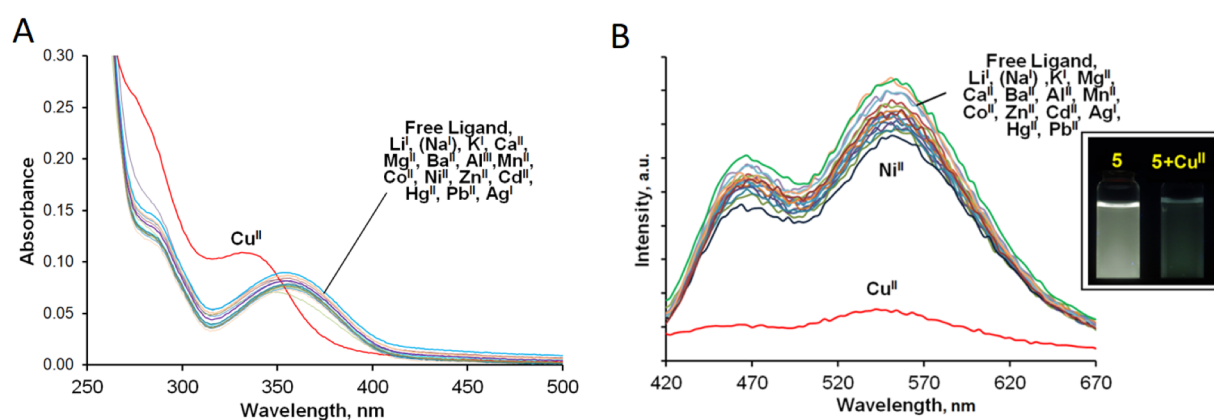


Figure 6. A) UV–vis spectra of **5** ($[5] = 27 \mu M$, 0.03M HEPES buffer, pH=7.4) before and after addition of 5 equiv of metal perchlorates. A) Fluorescence spectra of **5** ($[5] = 27 \mu M$, 0.03M HEPES buffer, pH=7.4, $\lambda_{ex} = 355$ nm) before and after addition of 5 equiv of metal perchlorates.

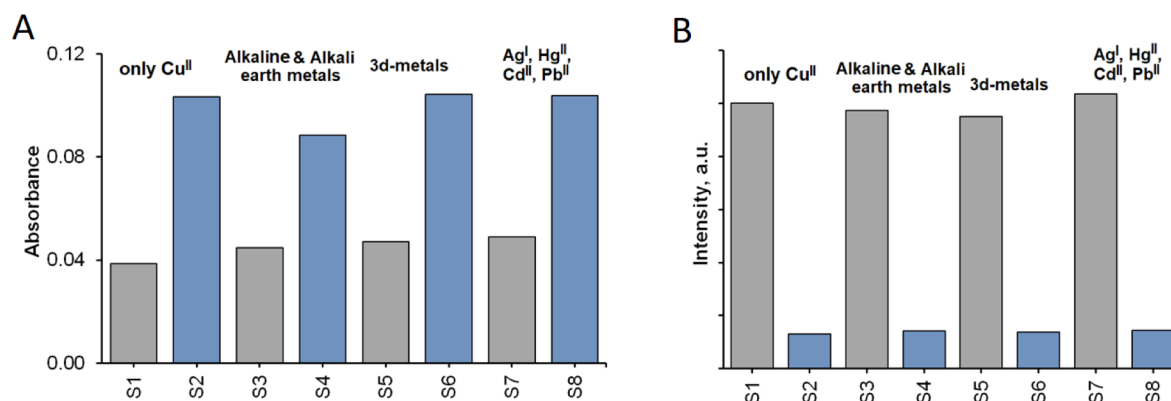


Figure 7. UV-vis (A, $\lambda = 318$ nm) and fluorescence (B, $\lambda = 550$ nm, $\lambda_{\text{ex}} = 355$ nm, intensity normalized to the ligand emission) cross-selectivity studies of metal ion binding by ligand **5** ($[\text{5}] = 27 \mu\text{M}$) in 0.03M HEPES buffer (pH=7.4). The spectral measurements were made for solution of ligand **5** (S1) without metal ions; (S2) after addition of Cu^{II} (1 equiv); (S3) after addition of Li^{I} , Na^{I} , K^{I} , Mg^{II} , Ca^{II} , Ba^{II} , Al^{III} (1 equiv of each metal ion); (S4) after addition of Li^{I} , Na^{I} , K^{I} , Mg^{II} , Ca^{II} , Ba^{II} , Al^{III} (1 equiv of each metal ion) and Cu^{II} (1 equiv); (S5) after addition of Mn^{II} , Co^{II} , Ni^{II} , Zn^{II} (1 equiv of each metal ion); (S6) after addition of Mn^{II} , Co^{II} , Ni^{II} , Zn^{II} (1 equiv of each metal ion) and Cu^{II} (1 equiv); (S7) after addition of Ag^{I} , Hg^{II} , Cd^{II} , Pb^{II} (1 equiv of each metal ion); (S8) after addition of Ag^{I} , Hg^{II} , Cd^{II} , Pb^{II} (1 equiv of each metal ion) and Cu^{II} (1 equiv).

Copper(II) ions can also be distinguished from other metal cations due to the fluorescence quenching which can be observed either visually or using a laboratory fluorometer (Fig. 6B). Although certain changes (less than 20%) of the emission intensity were effected by many metal ions, a strong and readily observable quenching of the emission (up to 80%) was noticed only in the presence of copper(II) ions. Competitive binding studies revealed that Cu^{II} could be effectively detected in the presence of other metal ions including Ag^{I} , Hg^{II} , Cd^{II} , Pb^{II} , Ni^{II} , Zn^{II} , Co^{II} at least when the concentration level of these metals is the same as that of Cu^{II} ions (Fig. 7). This selectivity can be explained by a higher affinity of ligand **5** to copper(II) ions compared to other metal ions because the observed response is independent on time.

The stability constant of Cu^{II} complex was determined by spectrophotometric and fluorimetric titrations of **5** with copper(II) perchlorate (Fig. S34 and 37). When Cu^{II} amount was gradually increased to 1.3 equiv, isobestic points were observed in the titration curves suggesting that only one spectrally distinct complex was formed in the studied solution. Numerical data processing was performed with Specfit program and the best fit was obtained when the titration curves were approximated by a 2-species (L-CuL) model to afford the value of $\log K_{11} = 5.85$. The calculated electronic

absorption spectra and distribution diagrams are displayed in Figs. S35 and S36. A similar value of stability constant ($\log K_{11} = 5.57$) was obtained by using a fluorescence titration data. The calculated emission spectra and distribution diagrams of the ligand **5** and the complex are shown in Figs. S38 and S39.

The limit of detection (LOD) of Cu^{II} ions has been determined by UV-vis and fluorescence spectroscopies using the 3σ method.⁴¹ Using a laboratory fluorometer, up to $0.3 \mu\text{M}$ of Cu^{II} ions can be detected what is significantly lower compared to spectrophotometric LOD which was found to be of $9 \mu\text{M}$. The action level of Cu^{II} ions in drinking water is fixed at $20 \mu\text{M}$ by EPA. Thus, ligand **5** is suitable for the analysis of drinking water by both optical detection methods. The choice of the method for the analysis of a real sample is determined by the concentration of the Cu^{II} ions and

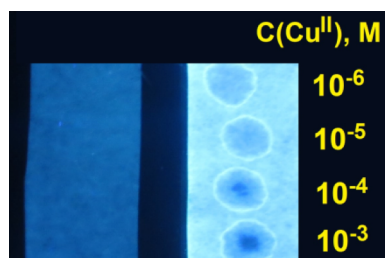


Figure 8. Left: filter paper used for preparation of test-strips. Right: Visual detection of Cu^{II} ions using test-strips based on ligand **5** under UV light.

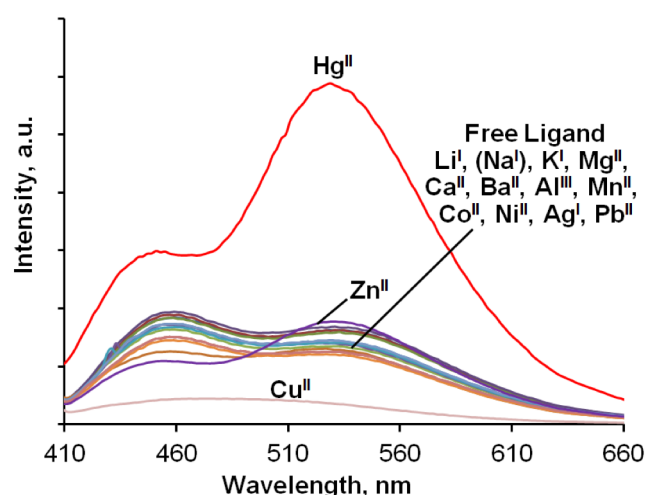


Figure 9. Fluorescence spectra of **6** ($[\text{6}] = 20 \mu\text{M}$, 0.03M HEPES buffer, pH=7.4, $\lambda_{\text{ex}} = 356$ nm) before and after addition of 1 equiv of metal perchlorates.

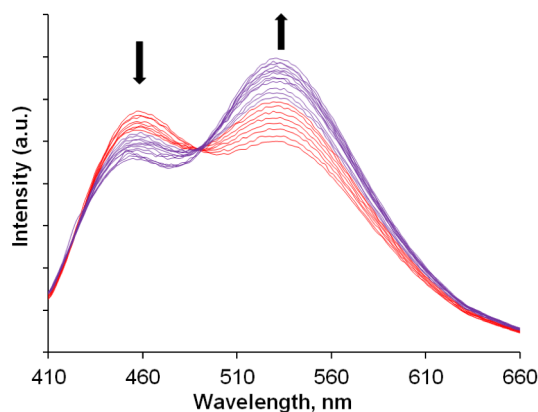


Figure 10. Fluorescence titration of ligand **6** ($[6] = 20 \mu\text{M}$, 0.03M HEPES buffer, $\text{pH}=7.4$, $\lambda_{\text{ex}} = 356 \text{ nm}$) upon addition of $\text{Zn}(\text{ClO}_4)_2$ (0–3 equiv).

the presence of other ions and small molecules which can perturbate the optical response of the chemosensor.

Chelator **5** appeared more sensitive and selective than the sensor **3** which is the only 6-aminoquinoline-derivative reported earlier for detection of Cu^{II} . Moreover, chelator **5** provides detection in aquatic media at physiological pH while chemosensor **3** was reported for sensing in acetonitrile.

We also prepared paper test-strips charged with the ligand **5** by wetting of filter papers with a CH_2Cl_2 solution of the ligand and drying them on air. Under UV-light, these strips enable a fast semi-quantitative determination of Cu^{II} ions at the ppm level and also can be used for the analysis of drinking water (Fig. 8).

The presence of the additional tertiary amine group in the molecule of the ligand **6** results in an increase of denticity and basicity of the ligand compared to chelator **5**. As a result, this ligand strongly binds not only Cu^{II} but also Hg^{II} and Zn^{II} cations, which is evidenced by changes in absorption in the presence of these metals (Fig. 9).

The ligand's emission decreased 5-fold in the presence of Cu^{II} ions (Figs. 9 and S43). When Hg^{II} ions (1 equiv) were added to the ligand solution, the peak intensity of fluorescence increased by 3.6 times and the maxima of two emission bands exhibited a blue shift (by 10 and 6 nm, respectively) (Figs. 9 and S45). In contrast, when the Zn^{II} /chelator ratio was gradually increased from 0 to 3, the isoemission point at 487 nm was observed (Fig. 10). Thus, ligand **6** can serve as a ratiometric fluorescent probe for Zn^{II} ions. The wavelengths of two maxima is convenient for the ratiometric measurements. Such a different response of emissive properties of ligand **6** in the presence of Hg^{II} , Cu^{II} and Zn^{II} ions could be used for identification of these ions.

These three metal ions can also be distinguished by using electronic absorption spectroscopy (Fig. S41). Addition of Hg^{II} , Cu^{II} and Zn^{II} salts leads to remarkable changes in the UV-vis spectrum of the chelator **6** being specific for each of them. Unfortunately, addition of other metal ions such as Pb^{II} , Co^{II} and Ni^{II} also influences the spectrum as shown in Fig. S41.

Next, the ligand **6** was titrated with Hg^{II} , Cu^{II} and Zn^{II} perchlorates to determine stability constants of their complexes by

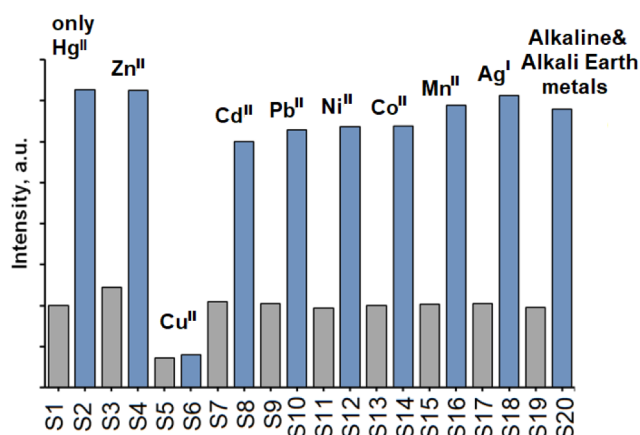


Figure 11. Fluorescence cross-selectivity studies of metal ion binding by ligand **6** ($[6] = 20 \mu\text{M}$) in 0.03M HEPES buffer ($\text{pH}=7.4$) at $\lambda = 550 \text{ nm}$ ($\lambda_{\text{ex}} = 356 \text{ nm}$). The spectral measurements were made for solution of ligand **6** (S1) without metal ions; (S2) after addition of Hg^{II} (1 equiv); (S3) after addition of Zn^{II} (1 equiv); (S4) **6** after addition of Zn^{II} (1 equiv), and Hg^{II} (1 equiv); (S5) after addition of Cu^{II} (1 equiv); (S6) after addition of Cu^{II} (1 equiv) and Hg^{II} (1 equiv); (S7) after addition of Cd^{II} (1 equiv); (S8) after addition of Cd^{II} (1 equiv) and Hg^{II} (1 equiv); (S9) after addition of Pb^{II} (1 equiv); (S10) after addition of Pb^{II} (1 equiv) and Hg^{II} (1 equiv); (S11) after addition of Ni^{II} (1 equiv); (S12) after addition of Ni^{II} (1 equiv) and Hg^{II} (1 equiv); (S13) after addition of Co^{II} (1 equiv); (S14) after addition of Co^{II} (1 equiv) and Hg^{II} (1 equiv); (S15) after addition of Mn^{II} (1 equiv); (S16) after addition of Mn^{II} (1 equiv) and Hg^{II} (1 equiv); (S17) after addition of Ag^{I} (1 equiv); (S18) after addition of Ag^{I} (1 equiv) and Hg^{II} (1 equiv); (S19) after addition of Li^{I} , Na^{I} , K^{I} , Mg^{II} , Ca^{II} , Ba^{II} , Al^{III} (1 equiv of each metal ion); (S20) after addition of Li^{I} , Na^{I} , K^{I} , Mg^{II} , Ca^{II} , Ba^{II} , Al^{III} (1 equiv of each metal ion) and Hg^{II} (1 equiv).

UV-vis and fluorescence spectroscopies (Figs. S3, 45 and S47). Isoestic points were observed in UV-vis titrations within the whole range of concentrations of added ions. This indicates that the only one spectrally distinct complex is formed in each of the studied solutions. However, calculations of the stability constants were successful only for $[\text{Zn}(\mathbf{6})]^{2+}$ because stability constants of other metal complexes were too high to be estimated by direct titration.⁴² The UV-vis- and fluorescence-based titration data for Zn^{II} complex were fitted to a 2-species ($\text{L}-\text{Zn}^{\text{II}}\text{L}$) model and the stability constant of $[\text{Zn}(\mathbf{6})]^{2+}$ was found to be $\log K_{11} = 5.1$ and 4.78 , respectively. The data for these titration experiments are shown in Figs. S47–S52. Job's plots based on UV-vis and fluorimetric data⁴³ of Hg^{II} and Cu^{II} complexes showed maxima for 1:1 molar ratio, thus establishing the 1:1 stoichiometry of complexes ratio in both experiments (Figs. S43–S46).

The investigations of the cross-selectivity of metal ion binding by fluorescence spectroscopy demonstrated that mercury ions could be determined in the presence of 14 different metals and only Cu^{II} ions strongly interfered with the detection (Fig. 11).

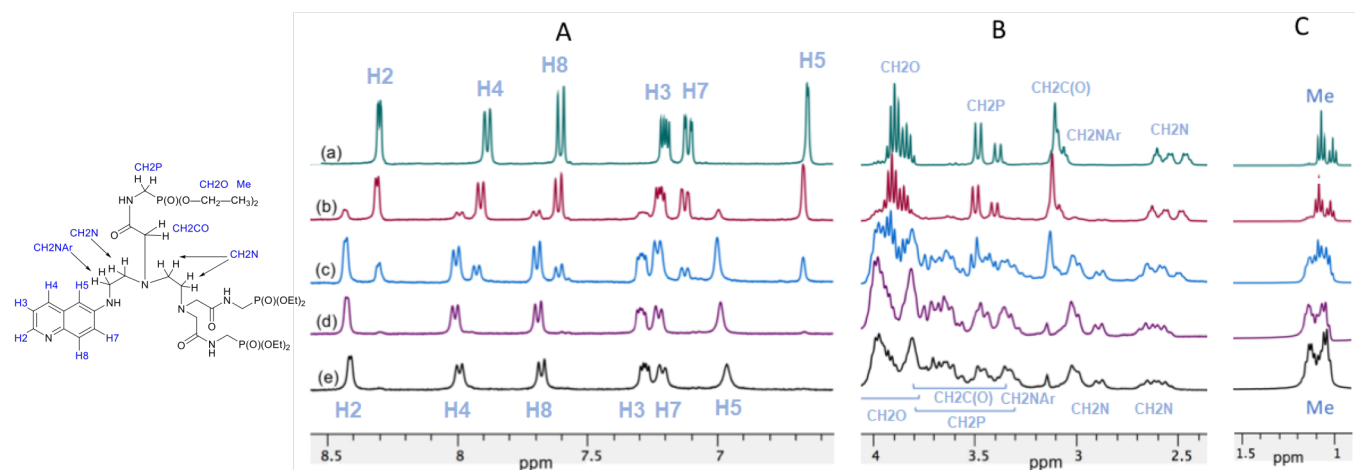


Figure 12. Aromatic (A) and aliphatic (B and C) regions of ^1H NMR spectrum (400 MHz) of **6** in D_2O -MeOD (5:1 v/v, $[\mathbf{6}] = 0.04 \text{ M}$) at 298 K before (a) and after addition of 0.2 (b), 0.6 (c), 1.0 (d) and 2.0 (e) equiv of zinc(II) perchlorate.

LOD of Hg^{II} ions was determined by using UV-vis and fluorescence techniques according to the 3σ method.⁴¹ In the UV-vis measurements, LOD was found to be of $3.0 \mu\text{M}$ (600 ppb), which can be significantly improved (40 nM, 8 ppb) using the emission measurements. Switch from UV-vis to fluorescence techniques also allows increase the working range of concentrations in which Hg^{II} ions can be detected by using chemosensor **6**.

It has to be noted, that LOD of Hg^{II} ions for colorimetric molecular probe **3**, the only one 6-aminoquinoline-based chemosensor reported previously for analysis of Hg^{II} ions in acetonitrile, was much higher (360 ppb).

We also prepared paper test-strips based on the ligand **6** by immersing filter papers into a 1.3 mM CH_2Cl_2 solution of the ligand **6** and drying them on air. Under UV-light, aqueous solutions of Hg^{II} , Cu^{II} and Zn^{II} perchlorates induce slight but quite different hue of the indicator fluorescence paper that can be used for qualitative determination of these metal ions (Fig S53).

Finally, it is noteworthy that compounds **5** and **6** are likely to serve as a useful alternative to the commonly used Schiff-base chemosensors bearing aminoquinoline signalling groups, for instance compound **2**¹⁰. The Schiff-base chemosensors are known to be unstable under acidic and basic conditions. This instability induces the necessity to work with freshly prepared solutions or even more serious problems related to decomposition of chemosensors during the analysis of real-life samples. The amino-based chemosensors are more stable and allow avoid this problem.

Structural studies of complexes

Unfortunately, all our attempts to grow single crystals of studied complexes for X-ray diffraction analysis were unsuccessful. However, preliminary structural information on the nature of these species can be derived from their UV-vis, FT-IR, ^1H and $^{31}\text{P}\{^1\text{H}\}$ NMR spectra. The most unambiguous information was obtained for $[\text{Zn}(\mathbf{6})]^{2+}$ complex by means of NMR spectroscopy, because the signals of the aromatic protons in **6** remained sharp during stepwise addition of zinc perchlorate allowing for accurate assignment of signals (Fig. 12).

Metal binding resulted in substantial spectral changes, especially in the high field region. Two distinct sets of signals corresponding to the free ligand **6** and complex $[\text{Zn}(\mathbf{6})]^{2+}$ were observed in the spectra. When 2 equiv of the metal salt were added to the ligand solution, the ^1H and $^{31}\text{P}\{^1\text{H}\}$ NMR spectra revealed the presence of only a single complex species (Figs. 12 and S54-S60). The proton signal assignment in this complex relies on ^1H - ^1H COSY, ^1H - ^1H NOESY and various NMR experiments with heteronuclear correlations (Table S1, Figs. S59-S67). To precise, using HSQC ^1H and ^{13}C chemical shifts as well as J_{PC} coupling constants were established, TOCSY experiment was used for the assignment of the signals in the triamine chain, NOESY helped to identify carbonyls in amido groups and adjacent methylene groups, while LR-HSQMBC was helpful in the correlation between phosphorus atoms and attached chelators. Also the analogies with the reference spectra for related polyamine-containing complexes were taken into consideration.³⁹ The summary of these data are also depicted in Fig. 12. According to the proton chemical shifts and their splitting pattern, the coordination environment of the zinc ion is formed by chelate rings. The three nitrogen atoms of the polyamine backbone together with the three amide groups are likely to be involved in binding Zn^{II} ion.

Additional information on the coordinated amide groups was gained from 1500–1700 cm^{-1} region of FT-IR spectrum, where the amide I ($\nu_{\text{C=O}} = 1669 \text{ cm}^{-1}$) and amide II ($\delta_{\text{CNH}} = 1521 \text{ cm}^{-1}$) bands of the free ligand **6** were observed (Figs. S60). Vibration frequency $\nu_{\text{C=O}}$ is diagnostic for the level of π -electron delocalization, and appear in 1615–1625 cm^{-1} region for metal-coordinated carbonyl oxygen atom of amide group.⁴⁴ In contrast, the formation of a deprotonated nitrogen-metal bands would result in a shift of $\nu_{\text{=O}}$ up to 1580 cm^{-1} partially overlapping with the δ_{CNH} bending band.⁴⁴ In the studied zinc complex the stretching $\nu_{\text{C=O}}$ band appeared at 1635 cm^{-1} indicating that the oxygen atom of the amide group was coordinated to the metal atom.

To gain deeper insights into the structure of complex $[\text{Zn}(\mathbf{6})]^{2+}$ and its electronic and photophysical properties DFT studies were performed. The structure of complex was modelled performing DFT

calculations using Firefly quantum chemistry package,⁴⁵ which is partially based on the GAMESS (US)⁴⁶ source code. The calculations were performed using B3LYP functional with STO 6-31G(d,p) basis set for all elements, at each step full optimization of geometry was achieved, and the minima were confirmed by computation of vibration frequencies. The modelling was started with computing the geometry of *N*-(6-quinolyl)-1,2-diaminoethane complex with Zn^{II} ion, and further, the other chelation centers were added one by one. This procedure gave the expected 6-coordinated Zn complex, in which Zn atom was bonded to three amine nitrogen atoms (one aromatic and two aliphatic amine centers), and three oxygen atoms of the amide groups. Two possible geometries were thus evaluated, and Fig. 13 shows the geometries of backbones of these complexes omitting hydrogen atoms and phosphonate-substituted arms. The complexes are deliberately displayed in a way revealing the close similarity of coordination environments and chelate rings.

Both geometries are similar to be composed of five chelate rings exhibiting no significant steric congestion in any part of the complex; the quinoline residue is bent outward in both complexes avoiding close contacts with the atoms of the polyamine scaffold. The main difference of the obtained configurations is in the relative positions of oxygen and nitrogen coordination centers. In the first configuration each oxygen center is opposed by amine nitrogen center in *trans*-geometry. In the second, there are *trans*-NN and *trans*-OO pairs and a single *trans*-NO pair. As far as there is no significant strain involved the difference between these complexes is likely to be accounted for by these *trans*-interactions, making the second complex marginally more stable (the difference between computed enthalpies of formation is only 1 kcal/mole in favour of the second complex) in agreement with slightly shorter bonds (e.g. the distance between Zn^{II} and heteroarylamine nitrogen is 2.10 Å vs 2.18 Å, etc.) in the second configuration. Such a close similarity of geometries and apparent lack of specific intramolecular interactions, along with marginal difference of energies makes these both configurations practically indistinguishable by spectral features, and we believe that both are formed in solutions under study. Fig. 14 shows the optimized geometry of the second complex

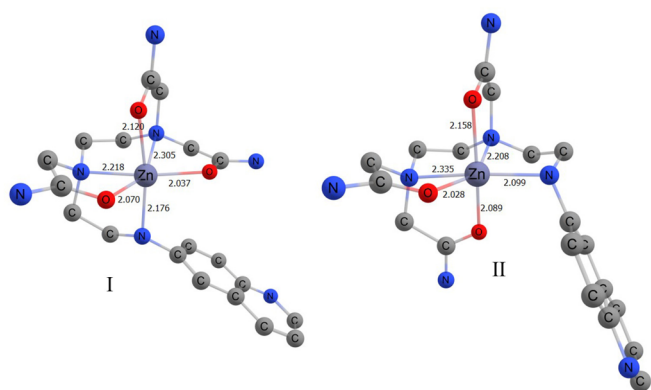


Figure 13. The geometries of model (hydrogen atoms and phosphonate pendant arms are omitted) Zn complexes of ligand **6** obtained by full geometry optimization at B3LYP/6-31G(d,p) level. The bond lengths of Zn atom with ligand centers are shown.

involving all phosphonate groups, revealing that highly polar P–O bonds are quite distant from the quinoline residue.

The elucidation of the coordination environment of Hg^{II} ions was much more difficult due to labile character of the complexes. Complex [Hg(**6**)]²⁺ was detected by ESI-HM analysis due to the presence of intensive peak at 566.66049 *m/z*. Metal binding produced also certain spectral changes in high and low field regions of ¹H NMR spectrum of the ligand **6** but all proton signals were broadened when 40 mM solution of the free ligand in D₂O/MeOH-*d*₄ (5:1) solvent mixture was titrated with the mercury(II) perchlorate (Fig. S60). The proton resonances from methyl groups of diethoxyphosphoryl substituents were easily recognized due to their characteristic chemical shifts. The increased number of methyl signals compared to that observed in the spectrum of ligand **6** and complex [Zn(**6**)]²⁺ indicated that at least some of diethoxyphosphoryl groups are bound to Hg^{II} ions. Upfield shift of the resonance of the aromatic proton H-5 was consistent with a coordination of the metal ion to the heteroarylamine nitrogen atom.

³¹P{¹H} NMR spectra afforded additional information on the complexes (Fig S60). After addition of 1 equiv of Hg^{II} perchlorate, three sets of phosphorous signals in approximate ratio of 2:2:1 were observed reflecting the presence of three different complexes in the solution. Each sets of signals was composed of three equal singlets. When the second equivalent of the mercury(II) perchlorate was added to the studied solution, the ratio of the complexes was changed and two major species were observed in the solution. In FT-IR spectrum of the evaporated solution (Hg^{II}/**6** ratio is 2/1), a very broad absorption band was observed at 1530–1660 cm⁻¹ that presumably could indicate that different coordination modes of amide group are observed in these Hg^{II} complexes and not all of them are coordinated to the metal centre.

It should be also noted, that only one complex was detected by UV-vis and fluorescence spectroscopies in more dilute (20–30 μM) solutions of chelator **6** after addition of the mercury(II) perchlorate. Thus, only one of three species detected by ³¹P{¹H} NMR spectroscopy in 0.04 M solution is sufficient stable to be observed in more diluted solutions by optical methods. Unfortunately, the

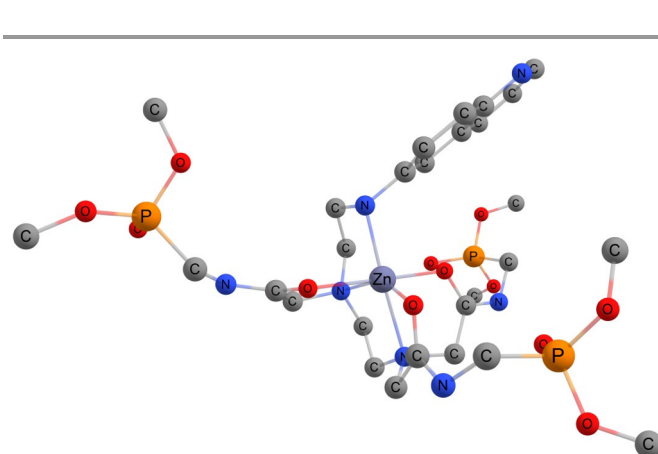


Figure 14. The optimized geometry (B3LYP/6-31G(d,p)) of methyl analogue of Zn complex with ligand **6**, all atoms except hydrogens are shown.

structure of this species cannot be determined by using NMR spectroscopy due to its labile character.

Paramagnetic character of Cu^{II} ions also makes the structural analysis of copper(II) complexes formed with ligand **6** difficult. The UV-vis response on Cu^{II} binding should result from the binding of Cu^{II} to the heterocyclic nitrogen atom or the aromatic amino group. The blue shift of the absorption maximum presumably indicates that the heteroarylamine nitrogen is coordinated to the metal centre. In 1500–1700 cm⁻¹ region of FT-IR spectrum, the two intensive bands are observed in the region of 1680–1600 cm⁻¹. They were assigned to amide I bands of free (1653 cm⁻¹) and coordinated by the oxygen atom (1624 cm⁻¹) amide groups. Based on a high affinity of Cu^{II} ions to aliphatic amines and typical coordination numbers of this metal ion, we can assume that three nitrogen atoms of the polyamine chain are involved in the complex formation and two amide groups complete the coordination sphere of the pentacoordinated metal centre.

Detection of sulfide anions

In view of the known high affinity of sulfide to Cu^{II} ions, many non-fluorescent copper complexes involving emissive ligands exhibit the appearance of fluorescent response in the presence of sulphides, which is quite useful for indirect detection of this anion in aqueous media.^{19b,47} The complex [Cu(**5**)]²⁺ can also be used for this purpose as shown in Fig. S76. Addition of excess (50 equiv) of sulphide to the solution of [Cu(**5**)]²⁺ in 0.03 M HEPES solution (pH = 7.4) led to a remarkable increase in the emission of the solution (about 4.2 times) which can be observed visually under UV irradiation of the solution.

Experimental

Materials and instruments

Unless otherwise noted, all chemicals and starting materials were obtained commercially from Acros® or Aldrich® and used without further purification. (1,4,7,10-Tetraazacyclotridecan-5-yl)methanamine (**2f**) was kindly provided by CheMatech (France). [(Bromoacetyl amino)methyl]phosphonic acid diethyl ester (**1**) was prepared according to published procedure.⁴⁸ Pd(dba)₂ was synthesized according to a known method and used without recrystallization.⁴⁹ The solvents were dried according standard procedures: dioxane was distilled successively over NaOH and sodium under argon, CH₂Cl₂ and CH₃CN were distilled over CaH₂, chloroform was distilled over P₂O₅. All reactions were performed in argon.

Column chromatography purification was carried out on silica gel (40–60 μm, Merck®).

UV-vis spectra were obtained with Varian Cary 60 spectrophotometer by using a rectangular quartz cell (Hellma, 111-QS, pathlength 10 mm, chamber volume: 3.5 mL). NMR spectra were acquired using Bruker Avance 400 MHz and Agilent 400MR spectrometers and referenced to solvent residual protons. MALDI-TOF mass-spectra were obtained with Bruker Daltonics Autoflex II mass-spectrometer in positive ion mode with dithranol matrix and polyethyleneglycols as internal standards. FT-IR spectra were registered with FT-IR Nexus (Nicolet) and Bruker Vector 22 spectrophotometers with Micro-ATR accessory (Pike). Accurate

mass measurements (HRMS ESI) were made using THERMO LTQ Orbitrap Elite. Solutions in methanol were used for the analysis. Fluorescence spectroscopic studies were performed with HORIBA Jobin Yvon Fluoromax-2 spectrophotometer with a standard fluorometer cell (Hellma, 111-QS, pathlength 10 mm, chamber volume: 3.5 mL). Emission spectra were recorded after excitation at the corresponding wavelength (excitation slit = 3 nm and emission slit = 3 nm).

Fluorescence quantum yields were measured at 25 °C by a relative method using quinine sulfate in 0.05 M H₂SO₄ (Φ_F = 54%) as a standard.⁵⁰ The following equation was used to determine the relative fluorescence quantum yield:

$$\phi_F = \phi_F^S \frac{F * A^S * n^2}{F^S * A * n_s^2}$$

where *A* is the absorbance (in the range of 0.01–0.1 a.u.), *F* is the area under the emission curve, *n* is the refractive index of the solvents (at 25 °C) used for the measurements, and the subscript *s* represents the standard. The following refractive index values are used: 1.333 for water and 1.341 for CH₃CN.

Synthesis

Synthesis of 8c. The solution of KOH (3.4 g, 61 mmol) in methanol (25 mL) was added to the solution of **8c**•2HCl (1.67 g, 7.62 mmol) in methanol (25 mL). The mixture was stirred for 1 h at room temperature, then 25 mL of dichloromethane was added to the reaction mixture. The solution was filtered, the filtrate was evaporated under reduced pressure and 50 mL of dichloromethane was added to the residue. The solution was again filtered, the filtrate was concentrated and dried under reduced pressure giving the product as colorless oil. Yield 900 mg (81%). ¹H NMR (400 MHz, CDCl₃): δ = 1.37 (br. s, 6H, NH), 2.64 (t, *J* = 5.8 Hz, 4H, CH₂NH₂), 2.71 (s, 4H, CH₂NH), 2.77 (t, *J* = 5.8 Hz, 4H, CH₂NH). ¹³C NMR (100.6 MHz, CDCl₃): δ = 41.7 (2C, CH₂NH₂), 49.3 (2C, CH₂NH), 52.4 (2C, CH₂NH).

Palladium-catalyzed amination of 6-bromoquinoline with polyamines. General procedure. A flask flushed with dry argon and equipped with a magnetic stirrer and condenser was charged with 6-bromoquinoline (0.5 mmol), Pd(dba)₂ (4–8 mol%), the phosphine ligand (4.5–9 mol%), the appropriate polyamine **2a–f** (0.5–5 mmol), and absolute 1,4-dioxane (5 mL). Sodium *tert*-butylate (0.75 mmol) was added, and the mixture was stirred under reflux for 24 h, and then cooled down to room temperature. Solvent was evaporated under reduced pressure, and the residue was chromatographed (silica gel, CH₂Cl₂, then CH₂Cl₂/MeOH, from 200:1 to 3:1, then CH₂Cl₂/MeOH/NH₃(aq), from 100:20:1 to 10:4:1 v/v).

N-(quinolin-6-yl)ethane-1,2-diamine (9a).⁵¹ Compound **9a** was obtained from 6-bromoquinoline (104 mg, 0.5 mmol) and **8a** (300 mg, 5 mmol) in the presence of Pd(dba)₂ (12 mg, 4 mol%) and BINAP (14 mg, 4.5 mol%). Yield: 70 mg (75%); yellowish oil; chromatography (silica gel, CH₂Cl₂/MeOH/NH₃(aq), 100:20:1 v/v). ¹H NMR (400 MHz, CDCl₃): δ = 1.73 (br. s, 2H, NH₂), 3.02 (t, *J* = 5.5 Hz, 2H, CH₂NH₂), 3.28 (t, *J* = 5.5 Hz, 2H, CH₂NQ), 4.46 (br. s, 1H, NHQ), 6.70 (d, ⁴*J* = 2.5 Hz, 1H, H5(Q)), 7.13 (dd, 1H, *J* = 9.0 Hz, ⁴*J* = 2.5 Hz, 1H, H7(Q)), 7.25 (dd, *J* = 8.3 Hz, *J* = 4.2 Hz, 1H, H3(Q)), 7.86 (d, *J* = 9.0 Hz, 1H, H8(Q)), 7.90 (dd, *J* = 8.3 Hz, ⁴*J* = 1.5 Hz, 1H, H4(Q)), 8.59 (dd, *J* = 4.3, ⁴*J* = 1.5 Hz, 1H, H2(Q)). ¹³C NMR (100.6 MHz,

CDCl₃): δ = 40.5 (1C, CH₂NH₂), 45.8 (1C, CH₂NQ), 102.8 (1C, C7(Q)), 121.3 (1C, CH(Q)), 121.6 (1C, CH(Q)), 129.8 (1C, CH(Q)), 130.1 (1C, C4a(Q)), 133.9 (1C, CH(Q)), 142.8 (1C, C6(Q)), 145.8 (1C, C2(Q)), 146.3 (1C, C8a(Q)). HRMS (ESI): m/z calc. for C₁₁H₁₄N₃: 188.1188; found: 231.1186 [M+H]⁺.

N-[2-(quinolin-6-ylamino)ethyl]ethane-1,2-diamine (9b).

Compound **9b** was obtained from 6-bromoquinoline (104 mg, 0.5 mmol) and **8b** (155 mg, 1.5 mmol) in the presence of Pd(dba)₂ (12 mg, 4 mol%) and BINAP (14 mg, 4.5 mol%). Yield: 71 mg (62%); yellowish oil; chromatography (silica gel, CH₂Cl₂/MeOH/NH₃(aq), 100:20:1 v/v). v_{\max}/cm^{-1} 3295br (NH), 3056m, 2939m, 2881w, 2849w, 2828w, 1657s, 1623s, 1509m, 1467m, 1436m, 1382m, 1361m, 1245m, 1180m, 1152m, 1124m, 1106m, 1025m, 830m, 791m, 768m, 648m, 624m, 474m. ¹H NMR (400 MHz, CDCl₃): δ = 2.05 (3H, br. s, NH, NH₂), 2.71 (t, J = 5.7 Hz, 2H, CH₂N), 2.82 (t, J = 5.7 Hz, 2H, CH₂N), 2.93 (t, J = 5.7 Hz, 2H, CH₂N), 3.28 (t, J = 5.7 Hz, 2H, CH₂NQ), 4.64 (br. s, 1H, NHQ), 6.68 (d, ⁴ J = 2.5 Hz, 1H, H5(Q)), 7.12 (dd, 1H, J = 9.0 Hz, ⁴ J = 2.5 Hz, 1H, H7(Q)), 7.23 (dd, J = 8.3 Hz, J = 4.3 Hz, 1H, H3(Q)), 7.84 (d, J = 9.0 Hz, 1H, H8(Q)), 7.88 (d, J = 8.3 Hz, 1H, H4(Q)), 8.58 (d, J = 4.3, 1H, H2(Q)). ¹³C NMR (100.6 MHz, CDCl₃): δ = 41.4 (1C, CH₂NH₂), 43.3 (1C, CH₂NQ), 48.0 (1C, CH₂CH₂NQ), 51.7 (1C, CH₂CH₂NH₂), 102.7 (1C, C7(Q)), 121.2 (1C, CH(Q)), 121.5 (1C, CH(Q)), 129.9 (1C, CH(Q)), 130.0 (1C, C4a(Q)), 133.6 (1C, CH(Q)), 143.0 (1C, C6(Q)), 145.8 (1C, C2(Q)), 146.2 (1C, C8a(Q)). HRMS (MALDI-TOF): m/z calc. for C₁₃H₁₉N₄: 231.1610; found: 231.1562 [M+H]⁺.

N-2-([2-(quinolin-6-ylamino)ethyl]aminoethyl)ethane-1,2-diamine (9c).

Compound **9c** was obtained from 6-bromoquinoline (104 mg, 0.5 mmol) and **8c** (220 mg, 1.5 mmol) in the presence of Pd(dba)₂ (12 mg, 4 mol%) and BINAP (14 mg, 4.5 mol%). Yield: 54 mg (40%); yellowish oil; chromatography (silica gel, CH₂Cl₂/MeOH/NH₃(aq), 20:5:1 v/v). v_{\max}/cm^{-1} 3311br (NH), 2938m, 2825m, 1658s, 1624s, 1578m, 1509m, 1439m, 1382m, 1246m, 1180m, 1151m, 1125m, 1023s, 831s, 792m, 768m, 624m, 543m, 475m. ¹H NMR (400 MHz, CDCl₃): δ = 2.21 (br. s, 4H, NH, NH₂), 2.67 (t, J = 5.7 Hz, 2H, CH₂N), 2.78 (br. s, 4H, CH₂N), 2.80 (t, ³ J = 5.7 Hz, 2H, CH₂N), 2.95 (t, J = 5.7 Hz, 2H, CH₂N), 3.30 (t, J = 5.7 Hz, 2H, CH₂N), 4.72 (br. s, 1H, NHQ), 6.68 (d, ⁴ J = 2.5 Hz, 1H, H5(Q)), 7.13 (dd, 1H, J = 9.1 Hz, ⁴ J = 2.5 Hz, 1H, H7(Q)), 7.23 (dd, J = 8.2 Hz, J = 4.2 Hz, 1H, H3(Q)), 7.83 (d, J = 9.1 Hz, 1H, H8(Q)), 7.88 (d, J = 8.2 Hz, 1H, H4(Q)), 8.58 (dd, J = 4.2, ⁴ J = 1.3 Hz, 1H, H2(Q)). ¹³C NMR (100.6 MHz, CDCl₃): δ = 41.4 (1C, CH₂NH), 43.2 (1C, CH₂NQ), 48.1 (1C, CH₂N), 48.9 (2C, CH₂N), 51.8 (1C, CH₂CH₂NH₂), 102.8 (1C, C7(Q)), 121.3 (1C, CH(Q)), 121.6 (1C, CH(Q)), 130.1 (2C, CH(Q), C4a(Q)), 133.7 (1C, CH(Q)), 143.2 (1C, C6(Q)), 146.0 (1C, C2(Q)), 146.4 (1C, C8a(Q)). HRMS (MALDI-TOF): m/z calc. for C₁₅H₂₄N₅: 274.2032; found: 274.2058 [M+H]⁺.

N-[3-(quinolin-6-ylamino)propyl]propane-1,3-diamine (9d).

Compound **9d** was obtained from 6-bromoquinoline (104 mg, 0.5 mmol) and **8d** (197 mg, 1.5 mmol) in the presence of Pd(dba)₂ (12 mg, 4 mol%) and BINAP (14 mg, 4.5 mol%). Yield: 58 mg (45%); yellowish oil; chromatography (silica gel, CH₂Cl₂/MeOH/NH₃(aq), 100:20:1 v/v). v_{\max}/cm^{-1} 3292br (NH), 2936m, 2823m, 1623m, 1531m, 1468m, 1438m, 1381m, 1323m, 1245m, 1179m, 1123m, 1025s, 931m, 829s, 767m, 622m, 747m. ¹H NMR (400 MHz, CDCl₃): δ = 1.67 (quint, J = 6.9 Hz, 2H, CH₂CH₂CH₂), 1.86 (quint, J = 6.5 Hz,

2H, CH₂CH₂CH₂), 2.06 (br. s, 3H, NH, NH₂), 2.71 (t, J = 6.9 Hz, 2H, CH₂N), 2.78 (t, J = 6.5 Hz, 4H, CH₂N), 3.28 (t, J = 5.5 Hz, 2H, CH₂NQ), 4.90 (br. s, 1H, NHQ), 6.65 (d, ⁴ J = 2.5 Hz, 1H, H5(Q)), 7.07 (dd, 1H, J = 9.1 Hz, ⁴ J = 2.5 Hz, 1H, H7(Q)), 7.24 (dd, J = 8.2 Hz, J = 4.2 Hz, 1H, H3(Q)), 7.83 (d, J = 9.1 Hz, 1H, H8(Q)), 7.88 (d, J = 8.2 Hz, 1H, H4(Q)), 8.58 (dd, J = 4.2, ⁴ J = 1.5 Hz, 1H, H2(Q)). ¹³C NMR (100.6 MHz, CDCl₃): δ = 28.8 (1C, CH₂CH₂NQ), 33.3 (1C, CH₂CH₂NH₂), 40.4 (1C, CH₂NH₂), 43.0 (1C, CH₂NQ), 47.9 (1C, CH₂NHCH₂), 48.5 (1C, CH₂NHCH₂), 102.4 (1C, C7(Q)), 121.3 (1C, CH(Q)), 121.5 (1C, CH(Q)), 130.1 (1C, CH(Q)), 130.2 (1C, C4a(Q)), 133.6 (1C, CH(Q)), 143.1 (1C, C6(Q)), 145.8 (1C, C2(Q)), 146.5 (1C, C8a(Q)). HRMS (MALDI-TOF): m/z calc. for C₁₅H₂₃N₄: 259.1923; found: 259.1971 [M+H]⁺.

N-(2-aminoethyl)-N-[2-(quinolin-6-ylamino)ethyl]ethane-1,2-diamine (9e).

Compound **9e** was obtained from 6-bromoquinoline (104 mg, 0.5 mmol) and **8e** (220 mg, 1.5 mmol) in the presence of Pd(dba)₂ (12 mg, 4 mol%) and BINAP (14 mg, 4.5 mol%). Yield: 74 mg (57%); yellowish oil; chromatography (silica gel, CH₂Cl₂/MeOH/NH₃(aq), 20:5:1 v/v). v_{\max}/cm^{-1} 3296br (NH), 3049m, 2938m, 2822m, 1658m, 1623s, 1574m, 1516s, 1466m, 1381s, 1323m, 1294m, 1268m, 1244m, 1180m, 1150m, 1124m, 1026s, 934m, 830s, 789m, 768m, 732m, 699m, 648m, 624m, 548m, 474m, 404m, 375m. ¹H NMR (400 MHz, CDCl₃): δ = 2.59 (t, J = 5.7 Hz, 4H, CH₂N), 2.70–2.80 (m, 10H, CH₂N, NH₂), 3.22 (t, J = 5.7 Hz, 2H, CH₂NQ), 5.30 (br. s, 1H, NHQ), 6.65 (d, ⁴ J = 2.4 Hz, 1H, H5(Q)), 7.16 (dd, 1H, J = 9.1 Hz, ⁴ J = 2.4 Hz, 1H, H7(Q)), 7.22 (dd, J = 8.3 Hz, J = 4.3 Hz, 1H, H3(Q)), 7.82 (d, J = 9.1 Hz, 1H, H8(Q)), 7.87 (d, J = 8.3 Hz, 1H, H4(Q)), 8.58 (dd, J = 4.3, ⁴ J = 1.5 Hz, 1H, H2(Q)). ¹³C NMR (100.6 MHz, CDCl₃): δ = 39.6 (2C, CH₂NH₂), 41.6 (1C, CH₂NQ), 53.0 (1C, CH₂N), 56.7 (2C, CH₂N), 102.7 (1C, C7(Q)), 121.3 (1C, CH(Q)), 121.6 (1C, CH(Q)), 130.1 (1C, CH(Q)), 130.2 (1C, C4a(Q)), 133.6 (1C, CH(Q)), 143.1 (1C, C6(Q)), 145.3 (1C, C2(Q)), 146.6 (1C, C8a(Q)). HRMS (MALDI-TOF): m/z calc. for C₁₅H₂₄N₅: 274.2032; found: 274.1988 [M+H]⁺.

N-(1,4,7,10-tetraazacyclotridecan-5-ylmethyl)quinolin-6-amine (9f).

Compound **9f** was obtained from 6-bromoquinoline (104 mg, 0.5 mmol) and **8f** (108 mg, 0.5 mmol) in the presence of Pd(dba)₂ (24 mg, 8 mol%) and BINAP (28 mg, 9 mol%). Yield: 63 mg (37%); yellowish oil; chromatography (silica gel, CH₂Cl₂/MeOH/NH₃(aq), 20:5:1 v/v). v_{\max}/cm^{-1} 3279br (NH), 2932m, 2819m, 1659m, 1622s, 1592m, 1576m, 1537m, 1510m, 1493m, 1464m, 1436m, 1380m, 1327m, 1288m, 1269m, 1180m, 1123m, 1029s, 931m, 830s, 767m, 730m, 699m, 646m, 620m, 591m, 545m, 474m. ¹H NMR (400 MHz, CDCl₃): δ = 1.65–1.76 (m, 2H, CH₂CH₂CH₂), 2.55–2.90 (m, 18H, CH₂N), 2.90–2.98 (m, 1H, CHN), 3.20–3.30 (m, 2H, CH₂NQ), 4.72 (br. s, 1H, NHQ), 6.67 (d, ⁴ J = 2.6 Hz, 1H, H5(Q)), 7.13 (dd, 1H, J = 9.1 Hz, ⁴ J = 2.6 Hz, 1H, H7(Q)), 7.24 (dd, J = 8.3 Hz, ³ J = 4.3 Hz, 1H, H3(Q)), 7.83 (d, J = 9.1 Hz, 1H, H8(Q)), 7.89 (d, J = 8.3 Hz, 1H, H4(Q)), 8.59 (dd, J = 4.3, ⁴ J = 1.5 Hz, 1H, H2(Q)). ¹³C NMR (100.6 MHz, CDCl₃): δ = 28.4 (1C, CH₂CH₂CH₂), 45.3 (1C, CH₂N), 45.7 (1C, CH₂N), 47.3 (1C, CH₂N), 48.5 (1C, CH₂N), 48.9 (1C, CH₂N), 49.4 (1C, CH₂N), 49.7 (1C, CH₂N), 51.0 (1C, CH₂N), 55.8 (1C, CHN), 102.6 (1C, C7(Q)), 121.2 (1C, CH(Q)), 121.6 (1C, CH(Q)), 130.0 (1C, CH(Q)), 130.1 (1C, C4a(Q)), 133.6 (1C, CH(Q)), 143.0 (1C, C6(Q)), 145.8 (1C, C2(Q)), 146.6 (1C, C8a(Q)). HRMS (MALDI-TOF): m/z calc. for C₁₉H₃₁N₆: 343.26; found: 343.28 [M+H]⁺.

Compound 5. A flask equipped with a magnetic stirrer and condenser was charged with **9a** (65 mg, 0.35 mmol), [(2-bromoacetyl-amino)methyl]phosphonic acid diethyl ester **1** (221 mg, 0.77 mmol) and chloroform (8.5 ml). DIPEA (150 mg, 1.16 mmol) was added, and the mixture was stirred at 40°C for 48 h under argon; the solution was evaporated under vacuum and the residue was chromatographed (silica gel, CH₂Cl₂, then CH₂Cl₂/MeOH, 200:1 to 3:1 v/v). Yield: 105 mg (50%); yellowish oil; chromatography (silica gel, CH₂Cl₂-MeOH, 10:1 v/v). $\nu_{\max}/\text{cm}^{-1}$ 3269br (NH), 3048br, 2927br, 2849br, 1663m (C=O, amide I), 1604s, 1588s, 1543m (NH, amide II), 1508m, 1475m, 1423m, 1409m, 1376m, 1340m, 1301m (CN, amide III), 1272m, 1251m (P=O), 1202m, 1173w, 1139w, 1114w, 1102w, 1034m (POC), 977m (POC), 860m, 830m, 814m, 730m, 701m. ¹H NMR (400 MHz, CDCl₃): δ = 1.25 (t, J = 6.8 Hz, 12H, CH₃), 2.85–2.88 (m, 2H, CH₂N), 3.25 (br. s, 6H, CH₂NQ, CH₂C(O)), 3.54 (dd, ² J_{PH} = 11.5 Hz, J = 6.2 Hz, 4H, CH₂P(O)), 4.03 (dq, ³ J_{PH} = ³ J_{HH} = 6.8 Hz, 8H, CH₂OP), 5.79 (br. s., 1H, NHQ), 6.62 (d, ⁴ J = 2.4 Hz, 1H, H5(Q)), 7.20 (dd, 1H, J = 4.3 Hz, J = 8.2 Hz, 1H, H3(Q)), 7.36 (dd, J = 9.1 Hz, ⁴ J = 2.4 Hz, 1H, H7(Q)), 7.80 (d, J = 9.1 Hz, 1H, H8(Q)), 7.84 (d, J = 8.2 Hz, 1H, H4(Q)), 8.05 (br. m, 2H, NHC(O)), 8.59 (dd, J = 4.3, 1H, H2(Q)). ¹³C NMR (100.6 MHz, CDCl₃): δ = 16.4 (d, ³ J_{PC} = 6.0 Hz, 4C, CH₃), 34.4 (d, ¹ J_{PC} = 155.9 Hz, 2C, CH₂P(O)), 41.3 (1C, CH₂NQ), 54.7 (1C, CH₂N), 59.4 (2C, CH₂C(O)), 62.6 (d, ² J_{PC} = 6.4 Hz, 4C, CH₂OP), 102.4 (1C, C7(Q)), 121.2 (1C, CH(Q)), 122.1 (1C, CH(Q)), 129.8 (1C, CH(Q)), 129.9 (1C, C4a(Q)), 133.7 (1C, CH(Q)), 142.9 (1C, C6(Q)), 145.8 (1C, C2(Q)), 146.4 (1C, C8a(Q)), 170.1 (1C, C(O)). ³¹P{¹H} NMR (162.5 MHz, CDCl₃): δ = 23.8 (2P). HRMS (MALDI TOF): m/z calc. for C₂₅H₄₂N₅O₈P₂: 602.2507; found: 602.2515 [M+H]⁺.

Compound 6. A flask equipped with a magnetic stirrer and condenser was charged with **9b** (51 mg, 0.22 mmol), [(2-bromoacetyl-amino)methyl]phosphonic acid diethyl ester **1** (209 mg, 0.73 mmol) and chloroform (6.7 ml). DIPEA (128 mg, 0.99 mmol) was added, and the mixture was stirred at 40°C for 48 h under argon; the solution was evaporated under vacuum and the residue was chromatographed (silica gel, CH₂Cl₂, then CH₂Cl₂/MeOH, 200:1 to 3:1 v/v). Yield: 79 mg (42%); yellowish oil; chromatography (silica gel, CH₂Cl₂/MeOH, 10:1 v/v). $\nu_{\max}/\text{cm}^{-1}$ 3305br (NH), 3056vw, 2981w, 2929w, 2906w, 2831vw, 1669m (C=O, amid I), 1653m, 1623m, 1576w, 1533m (NH, amide II), 1521m, 1506m, 1456w, 1436w, 1387m, 1381m, 1368w, 1300w (CN, amid III), 1219m (P=O), 1161m, 1123m, 1097m, 1045m, 1019s (POC), 972s (POC), 829m, 804m, 768m, 731m, 679m, 668s, 649m, 617m. ¹H NMR (400 MHz, CDCl₃): δ = 1.30 (t, J = 6.8 Hz, 12H, CH₃), 1.31 (t, J = 6.8 Hz, 6H, CH₃), 2.72–2.81 (m, 6H, CH₂N), 3.13 (br. s., 6H, CH₂C(O)), 3.22–3.24 (m, 2H, CH₂NQ), 3.70–3.84 (m, 6H, CH₂P(O)), 4.07–4.18 (m, 12H, CH₂OP), 5.69 (br. s, 1H, NHQ), 6.63 (d, ⁴ J = 2.5 Hz, 1H, H5(Q)), 7.28 (dd, 1H, J = 4.3 Hz, J = 8.4 Hz, 1H, H3(Q)), 7.49 (dd, J = 9.1 Hz, ⁴ J = 2.5 Hz, 1H, H7(Q)), 7.86 (d, J = 9.1 Hz, 1H, H8(Q)), 7.85 (d, J = 8.4 Hz, 1H, H4(Q)), 8.54–8.59 (m, 4H, H2(Q), NHC(O)). ¹³C NMR (100.6 MHz, CDCl₃): δ = 16.4 (d, ³ J_{PC} = 6.0 Hz, 6C, CH₃), 34.2 (d, ¹ J_{PC} = 156.0 Hz, 1C, CH₂P(O)), 34.5 (d, ¹ J_{PC} = 156.0 Hz, 2C, CH₂P(O)), 40.6 (1C, CH₂NQ), 52.1 (1C, CH₂N), 53.2 (1C, CH₂N), 54.2 (1C, CH₂N), 57.1 (1C, CH₂C(O)), 58.5 (2C, CH₂C(O)), 62.6 (d, ² J_{PC} = 6.6 Hz, 4C, CH₂OP), 62.8 (d, ² J_{PC} = 6.6 Hz, 2C, CH₂OP), 102.1 (1C, C7(Q)), 121.3 (1C, CH(Q)), 122.8 (1C, CH(Q)), 128.7 (1C, CH(Q)), 130.4 (1C, C4a(Q)), 134.6 (1C, CH(Q)), 140.3 (1C, C8a(Q)), 144.7 (1C, C6(Q)), 147.1 (1C, C2(Q)),

189.9 (3C, C(O)). ³¹P{¹H} NMR (162.5 MHz, CDCl₃): δ = 23.5 (2P), 23.6 (1P). HRMS (MALDI TOF): m/z calc. for C₃₄H₆₁N₇O₁₂P₃: 852.3591; found: 852.3539 [M+H]⁺.

***N,N*-bis(pyridin-2-ylmethyl)-*N'*-quinolin-6-ylethane-1,2-diamine**

(10). A flask equipped with a magnetic stirrer and condenser was charged with **9a** (65 mg, 0.35 mmol), 2-(chloromethyl)pyridine hydrochloride (138 mg, 0.84 mmol), potassium iodide (4 mg, 0.02 mmol) and acetonitrile (2 mL). DIPEA (220 mg, 1.7 mmol) was added, and the mixture was stirred under reflux for 12 h under argon, and then cooled down to r.t.; 30 ml of CH₂Cl₂ was added, the solution was washed with water (2 × 20 ml), the organic layer was dried over Na₂SO₄, evaporated under vacuum, and the residue was chromatographed (silica gel, CH₂Cl₂, then CH₂Cl₂/MeOH, 200:1 to 3:1 v/v). Yield: 49 mg (38%); yellow oil; chromatography (silica gel, CH₂Cl₂-MeOH, 35:1 v/v). $\nu_{\max}/\text{cm}^{-1}$ 3330br (N-H), 3290w, 3052w, 3009w, 2923w, 2848w, 1671m, 1623m, 1589m, 1569m, 1510m, 1472m, 1433m, 1379m, 1265m, 1246m, 1179m, 1148m, 1122, 1032m, 994m, 931m, 829m, 763m, 633m, 473m, 404s. ¹H NMR (400 MHz, CDCl₃): δ = 2.94 (t, J = 5.5 Hz, 2H, CH₂N), 3.24 (t, J = 5.5 Hz, 2H, CH₂NQ), 3.91 (s, 4H, CH₂Py), 6.56 (d, ⁴ J = 2.5 Hz, 1H, H5(Q)), 7.10–7.16 (m, 3H, H7(Q), H5(Py)), 7.23 (dd, J = 8.3 Hz, J = 4.3 Hz, 1H, H3(Q)), 7.39 (d, J = 9.0 Hz, 1H, H3(Py)), 7.59 (td, J = 7.5 Hz, ⁴ J = 1.5 Hz, 1H, H4(Py)), 7.84–7.86 (m, 2H, H8(Q), H4(Q)), 8.56 (m, 3H, H2(Q), H6(Py)) (NH proton was not unambiguously assigned). ¹³C NMR (100.6 MHz, CDCl₃): δ = 41.3 (1C, CH₂N), 52.3 (1C, CH₂NQ), 60.2 (2C, CH₂Py), 102.4 (1C, C7(Q)), 121.2 (1C, CH(Q)), 121.8 (1C, CH(Q)), 122.2 (2C, CH(Py)), 123.2 (2C, CH(Py)), 129.8 (1C, CH(Q)), 130.2 (1C, C4a(Q)), 133.7 (1C, CH(Q)), 136.5 (2C, CH(Py)), 142.8 (1C, C6(Q)), 145.8 (1C, C2(Q)), 146.6 (1C, C8a(Q)), 149.1 (2C, C6(Py)), 159.0 (2C, C2(Py)). HRMS (MALDI TOF): m/z calc. for C₂₃H₂₄N₅: 370.2032; found: 370.1990 [M+H]⁺.

Spectroscopic measurements

All the solutions were prepared with double-deionized high-purity water (18.2 MΩ cm) obtained from a «Millipore Simplicity» apparatus. All metal salts used were perchlorates of general M(ClO₄)_n·xH₂O formula. CAUTION! Although no problems were experienced, perchlorate salts are potentially explosive when combined with organic ligands and should be manipulated with care and used only in very small quantities. The 10⁻²-10⁻³ M aqueous solutions of all perchlorates except Hg(ClO₄)₂ were prepared in order to prevent the influence of dilution on the recorded spectra. Hg(ClO₄)₂ was used as a 10⁻² M solution in acetonitrile to avoid the hydrolysis of the salt. 0.03 M HEPES buffer (pH = 7.4) was prepared in beaker by the addition of 10 M NaOH solution by droplets to 0.03 M standard solution of HEPES under pH control until pH achieved 7.4.

Spectrophotometric titrations

Determination of protonation constants. pH measurements were carried out using «Mettler Toledo» apparatus with combined electrode LE438. The electrode was calibrated with commercial buffers (pH = 4.01 and 7.00). Protonation studies were conducted in a glass beaker, equipped with magnetic stirrer and pH-electrode. Aliquots of acid or base were added manually through LLG-digital micropipette to polyamines **5**, **6** and **10** solutions of appropriate concentrations and containing potassium chloride (KCl, C = 0.1 M).

Experimental details for each experiment are detailed in the captions for the figures. The entire multiwavelength data sets comprising at least 20 spectra were decomposed into their principal components by factor analysis before adjusting the equilibrium constants and calculations of extinction coefficients or normalized fluorescence spectra by nonlinear least-squares analysis with the Specfit/32 program.^{38,52}

Determination of stability constants of complexes. Aliquots of metal salts were added manually with the help of a Hamilton syringe to solutions of the chelators **5** and **6** of appropriate concentrations. Experimental details for each experiment are detailed in the captions of the figures. The spectra were recorded at pH = 7.4 (0.03 M HEPES buffer). The entire multiwavelength data sets comprising at least 20 spectra were decomposed into their principal components by factor analysis before adjusting the equilibrium constants and calculations of extinction coefficients or normalized fluorescence spectra by nonlinear least-squares analysis with the Specfit/32 program.^{38,52} The calculation of stability constant were performed taken into account the stability constants for the hydrolysed metal ion species.

Preparation of test-strips

The stripes were performed from filtrate paper (GOST 12026-76, Russia) in size 10 x 50 mm. The stripe was dipped into the test-tube with the solution of the ligand (C = 1.3 mM) for 1 min, that dried on air. The droplets of different solutions were placed on the stripe, than the stripe was shown under UV-light lamp (365 nm).

Conclusions

A convenient synthetic approach to polyamines bearing chromogenic quinolin-6-yl residue has been developed. Being conducted in the presence of a relatively cheap and commercially available palladium precatalyst, chemoselective arylation of non-protected polyamines with 6-bromoquinoline afforded monoarylated derivatives when the reaction was performed with polyamines taken in excess. In contrast to previously reported copper-catalyzed heterocoupling of 6-bromoquinoline with polyamines, the scope of this chemoselective reaction is quite large and target products can be obtained in good yields (up to 75%).

Polyamines bearing quinolin-6-yl residue are of interest for development of chemosensors for environmental analysis and clinical diagnostics. The protonation or coordination of metal ions by such chelators may induce large changes of their absorptive and emissive properties because the signaling aromatic unit is directly attached to the polyamine ionophore. In addition, further *N*-functionalization of the polyamine unit can be used to turn solubility and sensing properties of 6-polyaminoquinolines with respect to toxic metal ions. This synthetic route is convenient for the preparation of small libraries of molecular probes in which both the polyamine unit and the additional donor sites in the substituents at the nitrogen atoms can be varied. Proof of this concept is the synthesis of novel chemosensors for selective detection of Cu^{II} and Hg^{II} ions under physiological conditions.

All obtained compounds **5**, **6** and **10** act as pH sensitive sensors responding to pH changes by the evolution of absorption and emission of their solutions. However, the nature of the substituent

at aliphatic amino groups is the key parameter for tuning solubility and sensing properties of 6-polyaminoquinolines with respect to toxic metal ions. Chelator **10** bearing 2-pinacolyl residues is insoluble in pure water and produces optical response for many metal ions in aqueous media. In contrast, chemosensor **5** containing carboxamide moieties are suitable for selective double-channel detection of Cu^{II} ions under biologically and environmentally relevant conditions (aqueous media at pH = 7.4). This compound demonstrates low LOD of cupric ions and is suitable for the analysis of drinking water.

Increasing the number of donor sites in the polyamine ionophore, the selectivity of amidophosphonate-substituted 6-polyaminoquinolines towards toxic metal ions can be turned. Chemosensor **6** is useful for a sensitive detection of Hg^{II} ions under physiological conditions. Among 15 different metal ions, only Cu^{II} ions strongly disturbs the analysis of mercury(II) cations. Moreover, chemosensor **6** is a rare receptor able to produce three different fluorescence responses on the presence of Hg^{II}, Cu^{II} and Zn^{II} ions in aqueous solution. Such chemosensors are of particular interest for a complex analysis of industrial wastes and environmental samples coming from contaminated regions.

Conflicts of interest

The authors declare no conflicts of interest.

Acknowledgements

This work was carried out in the frames of the International Associated French-Russian Laboratory of Macrocyclic systems and Related Materials (LIA LAMREM) of the Centre National de la Recherche Scientifique (CNRS) and the Russian Academy of Sciences (RAS). We thank the CNRS, Russian Foundation for Basic Researches (RFBR) (grant N 17-53-16012), the Conseil Régional de Bourgogne (program PARI II) for financial support. The authors thank Dr. Michel Mayer for helpful discussions on FT-IR data. The authors thank Dr. Yury K. Grishin for providing structural NMR studies. The authors wish to acknowledge Thermo Fisher Scientific, Inc., MS Analytica (Moscow, Russia), and Prof. A. Makarov (Thermo Fisher Scientific, Inc.) personally for providing mass spectrometry equipment for this work. The authors wish to acknowledge the use of the NMR equipment purchased within the M.V. Lomonosov Moscow State University Program of Development.

Notes and references

- 1 (a) *Fluorescent Chemosensors for Ion and Molecule Recognition*, Vol. 538, American Chemical Society, Washington, DC, 1993, pp.1-235; (b) A. W. Czarnik, *Chem. Biol.*, 1995, **2**, 423; (c) A. P. de Silva, H. Q. N. Gunaratne, T. Gunnlaugsson, A. J. M. Huxley, C. P. McCoy, J. T. Rademacher and T. E. Rice, *Chem. Rev.*, 1997, **97**, 1515-1566; (d) B. Valeur and I. Leray, *Coord. Chem. Rev.*, 2000, **205**, 3; (e) M. Formica, V. Fusi, L. Giorgi and M. Micheloni, *Coord. Chem. Rev.*, 2012, **256**, 170.
- 2 (a) L. A. Bakar, N. M. Amin and H. A. Zakari, *Procedia Environ. Sci.*, 2015, **30**, 222-227; (b) J. K. Schaefer, A. Szczuka and F. M. M. Morel, *Environ. Sci. Technol.*, 2014, **48**, 3007.
- 3 <http://www.epa.gov/mercury/exposure.htm> (accessed February 2019).
- 4 C. J. Frederickson, J.-Y. Koh and A. I. Bush, *Nat. Rev. Neurosci.*, 2005, **6**, 449.
- 5 S. L. Sensi, P. Paoletti, A. I. Bush and I. Sekler, *Nat. Rev. Neurosci.*, 2009, **10**, 780.
- 6 V. Desai and S. G. Kaler, *Am. J. Clin. Nutr.*, 2008, **88**, 855S.
- 7 <https://www.epa.gov/eg/battery-manufacturing-effluent-guidelines-documents> (accessed February 2019).
- 8 M. A. Haque, V. Subramanian and R. J. Gibbs, *Crit. Rev. Environ. Control*, 1982, **12**, 13.
- 9 (a) P. Jiang and Z. Guo, *Coord. Chem. Rev.*, 2004, **248**, 205; (b) D. P. Selid, H. Xu, E. M. Collins, M. Striped Face-Collins and J. X. Zhao, *Sensors*, 2009, **9**, 5446; (c) D. T. Quang and J. S. Kim, *Chem. Rev.*, 2010, **110**, 6280; (d) I. Ratera, A. Tàrraga, P. Molina and J. Veciana, in *Organic Nanomaterials: Synthesis, Characterization, and Device Applications*, eds. T. Torres and G. Bottari, 2013, Chap. 24, p. 529-548; (e) X. Qian and Z. Xu, *Chem. Soc. Rev.*, 2015, **44**, 4487; (f) G. Chen, Z. Guo, G. Zeng and L. Tang, *Analyst*, 2015, **140**, 5400; (g) G. Sivaraman, M. Iniya, T. Anand, N. G. Kotla, O. Sunnapu, S. Singaravadiivel, A. Gulyani and D. Chellappa, *Coord. Chem. Rev.*, 2018, **357**, 50; (h) S. Suganya, S. Naha and S. Velmathi, *ChemistrySelect*, 2018, **3**, 7231.
- 10 (a) B. Nisar Ahmed, I. Ravikumar and P. Ghosh, *New J. Chem.*, 2009, **33**, 1825; (b) M. Alfonso, A. Tàrraga and P. Molina, *J. Org. Chem.*, 2011, **76**, 939; (c) J.-W. Oh, T. H. Kim, S. W. Yoo, Y. O. Lee, Y. Lee, H. Kim, J. Kim and J. S. Kim, *Sens. Actuators B-Chem.*, 2013, **177**, 813; (d) S. Madhu, D. K. Sharma, S. K. Basu, S. Jadhav, A. Chowdhury and M. Ravikanth, *Inorg. Chem.*, 2013, **52**, 11136; (e) T. Zhang, G. She, X. Qi and L. Mu, *Tetrahedron*, 2013, **69**, 7102; (f) P. Molina, A. Tàrraga and M. Alfonso, *Dalton Trans.*, 2014, **43**, 18; (g) Y. Liu, Q. Teng, J. Hu, R. Sun and H. Zhang, *Sens. Actuators B-Chem.*, 2016, **234**, 680-690; (h) Y. Fang, Y. Zhou, Q. Rui and C. Yao, *Organometallics*, 2015, **34**, 2962; (i) A. Hazra, A. Roy, A. Mukherjee, G. P. Maiti and P. Roy, *Dalton Trans.*, 2018, **47**, 13972.
- 11 T. Michinobu, Y. Li and T. Hyakutake, *Phys. Chem. Chem. Phys.*, 2013, **15**, 2623.
- 12 (a) E. Ranyuk, C. M. Douaihy, A. Bessmertnykh, F. Denat, A. Averin, I. Beletskaya and R. Guillard, *Org. Lett.*, 2009, **11**, 987; (b) A. S. Abel, A. Y. Mitrofanov, Y. Rousselin, F. Denat, A. Bessmertnykh-Lemeune, A. D. Averin and I. P. Beletskaya, *ChemPlusChem*, 2015, **81**, 35.
- 13 C. Hu, V. Raja Solomon, P. Cano and H. Lee, *Eur. J. Med. Chem.*, 2010, **45**, 705.
- 14 (a) R. Cheng, Y. Liu, S. Ou, Y. Pan, S. Zhang, H. Chen, L. Dai and J. Qu, *Anal. Chem.*, 2012, **84**, 5641; (b) S. K. Rastogi, P. Pal, D. E. Aston, T. E. Bitterwolf and A. L. Branen, *ACS Appl. Mat. Interfaces*, 2011, **3**, 1731.
- 15 (a) G. Pourfallah and X. Lou, *Dyes Pigm.*, 2018, **158**, 12; (b) B. K. Datta, S. Mukherjee, C. Kar, A. Ramesh and G. Das, *Anal. Chem.*, 2013, **85**, 8369; (c) Z. Dong, Y. Guo, X. Tian and J. Ma, *J. Lumin.*, 2013, **134**, 635.
- 16 J.-F. Zhu, H. Yuan, W.-H. Chan and A. W. M. Lee, *Tetrahedron Lett.*, 2010, **51**, 3550.
- 17 W.-J. Qu, J. Guan, T.-B. Wei, G.-T. Yan, Q. Lin and Y.-M. Zhang, *RSC Adv.*, 2016, **6**, 35804.
- 18 S. Patra, R. Gunupuru, R. Lo, E. Suresh, B. Ganguly and P. Paul, *New J. Chem.*, 2012, **36**, 988.
- 19 (a) A. Pramanik and G. Das, *Tetrahedron*, 2009, **65**, 2196; (b) K. G. Vaswani and M. D. Keränen, *Inorg. Chem.*, 2009, **48**, 5797; (c) Z. Dong, J. Jin, W. Zhao, H. Geng, P. Zhao, R. Li and J. Ma, *Appl. Surf. Sci.*, 2009, **255**, 9526; (d) J. Kang, S. P. Jang, Y.-H. Kim, J. H. Lee, E. B. Park, H. G. Lee, J. H. Kim, Y. Kim, S.-J. Kim and C. Kim, *Tetrahedron Lett.*, 2010, **51**, 6658; (e) L. Tang, P. Zhou, Z. Huang, J. Zhao and M. Cai, *Tetrahedron Lett.*, 2013, **54**, 5948; (f) X. Jia, X. Yu, X. Yang, J. Cui, X. Tang, W. Liu and W. Qin, *Dyes Pigm.*, 2013, **98**, 195; (g) L. Zhang, J. Sun, S. Liu, X. Cui, W. Li and J. Fang, *Inorg. Chem. Commun.*, 2013, **35**, 311; (h) P. Khakhlyar and J. B. Baruah, *Inorg. Chim. Acta*, 2016, **440**, 53; (i) L. Wang, J. Jin, L. Zhao, H. Shen, C. Shen and P. Zhang, *Carbohydr. Res.*, 2016, **433**, 41; (j) S. Zeng, S.-J. Li, X.-J. Sun, M.-Q. Li, Y.-Q. Ma, Z.-Y. Xing and J.-L. Li, *Spectrochim. Acta A*, 2018, **205**, 276.
- 20 (a) E. M. Nolan, J. Jaworski, K.-I. Okamoto, Y. Hayashi, M. Sheng and S. J. Lippard, *J. Am. Chem. Soc.*, 2005, **127**, 16812; (b) Y. Zhang, X. Guo, W. Si, L. Jia and X. Qian, *Org. Lett.*, 2008, **10**, 473; (c) N. Zhang, Y. Chen, M. Yu and Y. Liu, *Chem. – Asian J.*, 2009, **4**, 1697; (d) X. Zhou, B. Yu, Y. Guo, X. Tang, H. Zhang and W. Liu, *Inorg. Chem.*, 2010, **49**, 4002; (e) G. Xie, P. Xi, X. Wang, X. Zhao, L. Huang, F. Chen, Y. Wu, X. Yao and Z. Zeng, *Eur. J. Inorg. Chem.*, 2011, **2011**, 2927; (f) T. Liu and S. Liu, *Anal. Chem.*, 2011, **83**, 2775; (g) X. Tian, X. Guo, L. Jia, R. Yang, G. Cao and C. Liu, *Sens. Actuators B-Chem.*, 2015, **221**, 923; (h) X. Zhou, Y. Lu, J.-F. Zhu, W.-H. Chan, A. W. M. Lee, P.-S. Chan, R. N. S. Wong and N. K. Mak, *Tetrahedron*, 2011, **67**, 3412; (i) M.-h. Yan, T.-r. Li and Z.-y. Yang, *Inorg. Chem. Commun.*, 2011, **14**, 463; (j) Y. Ma, F. Wang, S. Kambam and X. Chen, *Sens. Actuators B-Chem.*, 2013, **188**, 1116.
- 21 (a) Y. Wan, W. Niu, W. J. Behof, Y. Wang, P. Boyle and C. B. Gorman, *Tetrahedron*, 2009, **65**, 4293-4297; (b) P. Kaur, H. Kaur and K. Singh, *RSC Adv.*, 2013, **3**, 64.
- 22 (a) S. G. Schulman, K. Abate, P. J. Kovi, A. C. Capomacchia and D. Jackman, *Anal. Chim. Acta*, 1973, **65**, 59; (b) A. Rajapakse, C. Linder, R. D. Morrison, U. Sarkar, N. D. Leigh, C. L. Barnes, J. S. Daniels and K. S. Gates, *Chem. Res. Toxicol.*, 2013, **26**, 555; (c) Y.-C. Cai, C. Li and Q.-H. Song, *ACS Sensors*, 2017, **2**, 834.
- 23 (a) W. Nashabeh and Z. El Rassi, *J. Chromatogr. A*, 1992, **600**, 279; (b) Y. Mechref, G. K. Ostrander and Z. El Rassi, *J. Chromatogr. A*, 1995, **695**, 83; (c) J. J. Wilson and J. S. Brodbelt, *Anal. Chem.*, 2008, **80**, 5186; (d) W. B. Struwe and P. M. Rudd, *Biol. Chem.*, 2012, **393**, 757.
- 24 M. Jonnada, G. D. El Rassi and Z. El Rassi, *Electrophoresis*, 2017, **38**, 1592.
- 25 F. Tanaka, R. Thayumanavan and C. F. Barbas, *J. Am. Chem. Soc.*, 2003, **125**, 8523.
- 26 (a) P. J. Brynes, P. Bevilacqua and A. Green, *Anal. Biochem.*, 1981, **116**, 408-413; (b) S. A. Cohen and D. P. Michaud, *Anal. Biochem.*, 1993, **211**, 279; (c) W. Huang, S. N. Hicks, J. Sondek and Q. Zhang, *ACS Chem. Biol.*, 2011, **6**, 223; (d) E. Danieli and D. Shabat, *Bioorg. Med. Chem.*, 2007, **15**, 7318.

- 27 (a) S. Halder, A. Hazra and P. Roy, *J. Lumin.*, 2018, **195**, 326; (b) S. Halder, S. Dey and P. Roy, *RSC Adv.*, 2015, **5**, 54873.
- 28 (a) D. W. Kim, J. Kim, J. Hwang, J. K. Park and J. S. Kim, *Bull. Korean Chem. Soc.*, 2012, **33**, 1159; (b) A. Dorazco-González, M. F. Alamo, C. Godoy-Alcántar, H. Höpfl and A. K. Yatsimirsky, *RSC Adv.*, 2014, **4**, 455; (c) I. J. Bazany-Rodríguez, D. Martínez-Otero, J. Barroso-Flores, A. K. Yatsimirsky and A. Dorazco-González, *Sens. Actuators B-Chem.*, 2015, **221**, 1348.
- 29 L. D. Chebrolu, S. Thurakkal, H. S. Balaraman and R. Danaboyina, *Sens. Actuators B-Chem.*, 2014, **204**, 480.
- 30 (a) L. Xue, G. Li, Q. Liu, H. Wang, C. Liu, X. Ding, S. He and H. Jiang, *Inorg. Chem.*, 2011, **50**, 3680; (b) Z. Liu, G. Li, Y. Wang, J. Li, Y. Mi, D. Zou, T. Li and Y. Wu, *Talanta*, 2019, **192**, 6.
- 31 A. S. Abel, A. D. Averin and I. P. Beletskaya, *New J. Chem.*, 2016, **40**, 5818-5828.
- 32 J. F. Callan, A. P. de Silva, J. Ferguson, A. J. M. Huxley and A. M. O'Brien, *Tetrahedron*, 2004, **60**, 11125.
- 33 M. Mei and S. Wu, *New J. Chem.*, 2001, **25**, 471.
- 34 S. Banthia and A. Samanta, *J. Phys. Chem. B*, 2006, **110**, 6437.
- 35 I. P. Beletskaya, A. G. Bessmertnykh and R. Guillard, *Tetrahedron Lett.*, 1997, **38**, 2287.
- 36 I. P. Beletskaya, A. D. Averin, A. G. Bessmertnykh, F. Denat and R. Guillard, *Russ. J. Org. Chem.*, 2010, **46**, 947.
- 37 M. V. Anokhin, A. D. Averin, S. P. Panchenko, O. A. Maloshitskaya and I. P. Beletskaya, *Mendeleev Commun.*, 2015, **25**, 245.
- 38 H. Gampp, M. Maeder, C. J. Meyer and A. D. Zuberbühler, *Talanta*, 1985, **32**, 257.
- 39 E. Ranyuk, A. Uglov, M. Meyer, A. B. Lemeune, F. Denat, A. Averin, I. Beletskaya and R. Guillard, *Dalton Trans.*, 2011, **40**, 10491.
- 40 B. A. Wong, S. Friedle and S. J. Lippard, *Inorg. Chem.*, 2009, **48**, 7009.
- 41 D. J. Anderson, *Clin. Chem.*, 1989, **35**, 2152.
- 42 Z. Slovák and J. Borák, *Anal. Chim. Acta*, 1974, **68**, 425.
- 43 P. MacCarthy, *Anal. Chem.*, 1978, **50**, 2165.
- 44 M. Meyer, L. Frémond, E. Espinosa, R. Guillard, Z. Ou and K. M. Kadish, *Inorg. Chem.*, 2004, **43**, 5572.
- 45 A. A. Granovsky, *Firefly version 8*, <http://classic.chem.msu.su/gran/firefly/index.html> (accessed February 2019).
- 46 M.W.Schmidt, K.K.Baldrige, J.A.Boatz, S.T.Elbert, M.S.Gordon, J.H.Jensen, S.Koseki, N.Matsunaga, K.A.Nguyen, S.Su, T.L.Windus, M.Dupuis and J.A.Montgomery, *J.Comput.Chem.*, 1993, **14**, 1347.
- 47 (a) L. Tang, P. Zhou, Z. Qi, Z. Huang, J. Zhao and M. Cai, *Bull. Korean Chem. Soc.*, 2013, **34**, 2256; (b) L. Tang, P. Zhou, Q. Zhang, Z. Huang, J. Zhao and M. Cai, *Inorg. Chem. Commun.*, 2013, **36**, 100; (c) C. Gao, X. Liu, X. Jin, J. Wu, Y. Xie, W. Liu, X. Yao and Y. Tang, *Sens. Actuators B-Chem.*, 2013, **185**, 125.
- 48 F. K. Kálmán, M. Woods, P. Caravan, P. Jurek, M. Spiller, G. Tircsó, R. Király, E. Brücher and A. D. Sherry, *Inorg. Chem.*, 2007, **46**, 5260.
- 49 T. Ukai, H. Kawazura, Y. Ishii, J. J. Bonnet and J. A. Ibers, *J. Organomet. Chem.*, 1974, **65**, 253.
- 50 A. M. Brouwer, *Pure Appl. Chem.*, 2011, **83**, 2213.
- 51 G. B. Behera, P. C. Rath and M. K. Rout, *J. Indian Chem. Soc.*, 1967, **44**, 119.
- 52 R. A. Binstead, B. Jung and A. D. Zuberbühler, *SPECFIT/32, Global Analysis System, ver 3.0; Spectrum Software Associates: Marlborough, USA*, 2000.